

RICE UNIVERSITY

**Improved Seismic Risk Assessment of Non-ductile Reinforced
Concrete Buildings**

by

Blaine Jacob Fuselier

A THESIS SUBMITTED
IN PARTIAL FULFILLMENT OF THE
REQUIREMENTS FOR THE DEGREE

Master of Science

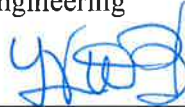
APPROVED, THESIS COMMITTEE



Jamie Padgett, Chair
Assistant Professor of Civil &
Environmental Engineering



Satish Nagarajaiah
Professor of Civil & Environmental
Engineering



Leonardo Duenas-Osorio
Associate Professor of Civil &
Environmental Engineering

HOUSTON, TEXAS
February 2014

ABSTRACT

Improved Seismic Risk Assessment of Non-ductile Reinforced Concrete Buildings

by

Blaine Jacob Fuselier

Existing reinforced concrete (RC) buildings built to non-ductile specifications are highly susceptible to damage given lateral loads induced from earthquake ground motions. To explore the effects of these ground motions, non-linear finite element analyses are being used in research and practice to model non-ductile RC buildings as well as conduct probabilistic analyses of their seismic fragility in as-built and retrofitted conditions. This study examines the influence of modeling fidelity on the response and fragility of non-ductile RC buildings, testing the role of explicitly capturing local failure in the finite element model. Beyond seismic response and fragility modeling, this thesis aims to address a current gap in consequence modeling and risk assessment of non-ductile RC buildings by characterizing the uncertainty in closure or tagging decisions resulting from damage to RC components. A survey is presented to assess the tagging decisions made by trained professionals during post-earthquake rapid evaluations of reinforced concrete buildings and compare these results to empirical data from past earthquake reconnaissance reports. The resulting models can support risk

assessment as well as provide an alternative basis for retrofit selection for deficient structures.

Acknowledgments

There are many people I would like to acknowledge who made this thesis a reality. First off, I need to thank my advisor, Dr. Jamie Padgett, for bringing me to Rice University in 2011. Her support and believing in me at all times helped me through my time at Rice and will continue to help me in my future endeavors. Next, I would like to thank my committee members, Dr. Satish Nagarajaiah and Dr. Leonardo Duenas-Osorio, for their guidance during my time at Rice University.

Next, I need to acknowledge the great project I was a part of with material based upon work supported by the National Science Foundation under grant number CMMI-1041607. I would like to thank the survey respondents. Mr. Laurence Kornfield and the San Francisco Department of Building Inspection are also appreciated for offering access to the Loma Prieta Earthquake tagging files discussed this study.

There are incredible people I need to thank who helped me during my time at Rice University, my friends: Candase Arnold, Jay Ghosh, Navid Ataei, Emily McCarthy, Citlali Tapia, Vahid Bisadi, Xoab Perez, and my international friends Fabio Freddi, Behzad Zakeri, and Mairead Ni Choine. Also, to my best buddy at Rice Akwasi Mensah. Finally, my family and wife, Amber, for supporting me to no end and always being there during good and bad times. Thank you all!

Contents

Acknowledgments	iv
Contents	v
List of Figures	vii
List of Tables	x
List of Equations	xi
Introduction	1
1.1. Motivation and Scope of Research	1
1.2. Organization of Thesis	5
Literature Review	6
2.1. Reinforced Concrete Buildings in Seismic Regions	6
2.1.1. Inventory of Non-Ductile Reinforced Concrete Buildings	6
2.1.2. Deficiencies in Non-Ductile Detailing	7
2.1.3. Typical Damage Observed in Reinforced Concrete Elements	7
2.2. Non-Linear Finite Element Modeling	8
2.2.1. Beam and Column Element Modeling	8
2.2.2. Joint Research	9
2.2.3. Uncertainties Associated with Seismic Analysis	9
2.3. Probabilistic Risk Assessment of Reinforced Concrete Buildings	11
2.4. Tagging Guidelines for Reinforced Concrete Buildings	12
Comparison of Modeling Strategies to Capture Component Level Damage in Non-ductile Reinforced Concrete Buildings	14
3.1. Introduction.....	14
3.2. Alternative Modeling Approaches	15
3.2.1. Case Study Structure	16
3.2.2. Rigid Model	18
3.2.3. Column Model	18
3.2.4. Joint Model	19
3.3. Model Comparisons with Experimental Data	20

3.3.1. Subassemblage Model.....	21
3.3.2. One-third Scale Model.....	24
3.4. Impact of Modeling Approach on Probabilistic Seismic Response Assessment	27
3.4.1. Probabilistic Seismic Demand Analysis of System and Components	27
3.4.1.1. Linear Regression Models	29
3.4.1.2. Bilinear Regression Models.....	30
3.4.2. PSDM Comparisons.....	34
3.4.3. Finite Element Model Uncertainty	36
3.5. Component Fragility Curves	40
Rapid Evaluation Survey of Earthquake Damaged Reinforced Concrete Components	44
4.1. Introduction.....	44
4.2. Web-based survey organization.....	46
4.3. Results	49
4.3.1. Demographic Analysis.....	49
4.3.2. Post-Earthquake Evaluation Tagging and Repairs	50
4.3.3. Comments.....	58
4.4. Comparison with Empirical Data	60
Conclusions and Future Research Opportunities	65
5.1. Summary and Conclusions	65
5.2. Future Research Recommendations	70
References	72
Appendix A	76
Appendix B.....	77
Appendix C.....	82

List of Figures

Figure 3.1 - OpenSees full-scale two-dimensional model with four different combinations of the joint and column spring details: a) rigid, b) column, c) joint, d) joint-column. Beam and column section detailing is referenced (Bracci et al. 1992a).	17
Figure 3.2 - Comparison of the rigid and joint models to experimental data for the interior subassemblage.....	23
Figure 3.3 - Comparison of the rigid and joint models to experimental data for the exterior subassemblage.	23
Figure 3.4 - 3rd story displacement data for comparing one-third experimental with rigid and joint-column models using dynamic analysis ground motion from Taft at PGA of 0.30g.....	24
Figure 3.5 - Rigid model PSDM for: a) maximum interstory drift at first floor, seen as linear; b) maximum moment at the interior column on first floor, seen as bilinear. Sd(T1) is used as the IM.....	31
Figure 3.6 - Bilinear PSDM for maximum shear at the interior column on the first floor in: a) rigid b) joint c) column and d) joint-column models. Sd(T1) is used as the IM.....	33
Figure 3.7 - Bilinear PSDM for maximum interior joint strain at the first floor in: a) joint and b) joint-column models. Sd(T1) is used as the IM.	33
Figure 3.8 - Scatterplot of calculated variation data of shear EDP vs. natural log of spectral displacement.	39
Figure 3.9 - Ultimate moment fragility curves for columns on first level; these fragility curves are calculated not including the σ_{FEM} uncertainty.....	43
Figure 3.10 - Ultimate moment fragility curves for columns on first level; these fragility curves are calculated including the σ_{FEM} uncertainty.	43
Figure 4.1- Screenshots of a typical section from the online survey, which includes: (a) images demonstrating one of five different types of component damage due to earthquakes (joint damage in this case) and (b) questions pertaining to the images. Examples of responses are depicted for the post-	

earthquake evaluation tagging and open-ended questions concerning repair possibilities, estimated time and cost of these repairs, preventative measures, and additional comments.....	48
Figure 4.2 - (a) An example of X-Cracking through a multi-story building column shown in the survey. (b) Probabilities of two column shear damage types receiving tags.....	52
Figure 4.3 - (a) An example of spalling on a column shown in the survey. (b) Probabilities of column and joint spalling receiving tags.	53
Figure 4.4 - (a) An example of rebar seen and buckling on a joint shown in the survey. (b) Probabilities of two joint damage types receiving tags.	54
Figure 4.5 - (a) An example of crushed concrete with rebar buckling at the base of a column shown in the survey. (b) Probabilities of two types of column flexure damage receiving tags.....	55
Figure 4.6 - (a) An example of flexural hinging in a beam shown in the survey. (b) Probability of two types of beam damage receiving tags.	56
Figure C.1 - Consent form for participation in survey.....	82
Figure C.2 - Personal information page in survey.	83
Figure C.3 - Reinforced concrete column shear, part one, in survey.	84
Figure C.4 - Reinforced concrete column shear, part two, in survey.	85
Figure C.5 - Reinforced concrete spalling of column in survey.....	86
Figure C.6 - Reinforced concrete spalling of joint in survey.	87
Figure C.7 - Reinforced concrete joint damage, part one, in survey.	88
Figure C.8 - Reinforced concrete joint damage, part two, in survey.	89
Figure C.9 - Reinforced concrete column flexure damage in survey.	90
Figure C.10 - Reinforced concrete story lean observed damage in survey.....	91
Figure C.11 - Reinforced concrete beam damage, part one, in survey.	92
Figure C.12 - Reinforced concrete beam damage, part two, in survey.	93

Figure C.13 - Reinforced concrete correlations between damages in survey. . 94

List of Tables

Table 3.1 - Dynamic characteristics of experimental vs. analytical modeling techniques; period values in parentheses are the natural periods observed in the experimental model after the Taft 0.05g, 0.20g, and 0.30g PGA ground motions.....	25
Table 3.2 - Local and global engineering demand parameters considered for probabilistic seismic demand models.....	28
Table 3.3 - T-test results comparing PSDM data from the four analytical models; (1) indicates existent relationship , whereas (0) indicates no relationship with 90 percent confidence.....	36
Table 3.4 - σ_{FEM} data for each EDP at values less and greater than $\ln(Sd(T1)) = -2.5$.	39
Table 3.5 - Limite State Capacities for use in fragility analysis	41
Table 4.1 - Experience of survey participants from different occupational backgrounds.	50
Table 4.2 - Suggested repairs from survey.....	61
Table 4.3 - Number of responses, duration (months), and costs (\$) of repairs with mean, median, and mode values.....	62
Table 4.4 - Tagging and damage data of RC structures after the Loma Prieta earthquake.	64
Table A.1 - Parameters used in the OpenSees limit state material, axial limit curve, and shear limit curve for the column model.	76
Table A.2 - Unloading and pinching point parameters to be defined in the Pinching4 uniaxial material for zero length element located at joint intersection.	76

List of Equations

Equation 3.1- Joint shear cracking stress	20
Equation 3.2 - Demand power model developed by Cornell et al. (2002)	29
Equation 3.3 - Linear representation of the power model in the log-log space...29	
Equation 3.4 - First linear regression in the bilinear model where $\ln(IM) \leq \ln(IM_{mid})$	30
Equation 3.5 - Second linear regression in the bilinear model where $\ln(IM) \geq \ln(IM_{mid})$	30
Equation 3.6 - Variation of demands between various finite element models	37
Equation 3.7 - Fragility expression.....	40

Chapter 1

Introduction

1.1. Motivation and Scope of Research

The study of non-ductile reinforced concrete (RC) buildings is important to consider for regions that observe earthquake activity. While non-ductile RC buildings are sufficient for gravity load design, they are susceptible to damage during earthquake events. These buildings are not up to code as compared to today's standards and codes, and they may show signs of damage under seismic loading to critical components such as the columns and joints. RC buildings designed today are strengthened in key elements and are designed with more ductility. These ductile requirements eliminate the brittle failures that are observed in non-ductile RC structures. The failures that arise in non-ductile RC buildings are accentuated because of the deficiencies in the design. These deficiencies are characterized by the amount of steel reinforcement and lap splice connections within the RC elements.

The columns and joints are the most critical elements in non-ductile RC buildings, which typically exhibit weak column-strong beam behavior. Past damage investigated in RC buildings is observed in the columns as shear, flexure, and spalling, and the joints as spalling and cracking failure. The beams do not show much damage following the weak column-strong beam relationship in non-ductile RC buildings.

Considering the typical damage areas identified in a non-ductile RC building, finite element models (FEMs) may be used to capture demands from the components in a RC building. The majority of studies on vulnerability modeling and risk assessment (e.g. probability of damage or impending consequences) of RC buildings in the past have performed risk assessments based on global engineering demand parameters (EDPs) such as drift, acceleration, and displacement (Bai, Gardoni, & Hueste, 2011; Ellingwood & Wen, 2005; Serdar Kircil & Polat, 2006). In fact, global EDPs are widely accepted in national risk assessment packages to predict damage in a building (FEMA, 2011). Component level demands captured for vulnerability modeling and risk assessment in RC buildings have more recently been assessed (Freddi, Padgett, & Dall'Asta, 2012). To evaluate the component level EDPs for a more thorough risk assessment, refined component level models may be incorporated into the FEMs to capture a more accurate response of the key areas of observed damage in non-ductile RC buildings. Based upon the EDPs gathered from the FEM simulation, fragility curves may be developed as demonstrated in this thesis using linear and bi-linear regression of the demand data that provide probabilistic models of component response given ground motion intensity. Upon

comparing these demands to component capacities, resulting fragility curves will further identify the most likely areas of failure in non-ductile RC buildings. Motivation in this study arises from the fact that there are various options in modeling used to assess the risk of non-ductile RC buildings. Past studies have their unique modeling approach and perspective for capturing data for a probabilistic response and risk assessment. These strategies may range from a simplistic FEM to a more sophisticated FEM by incorporating more advanced component models. The study presented in Chapter 3 provides direct comparisons of common local and global EDPs captured from a range of models varying in sophistication. Furthermore uncertainty in response prediction attributed to variation in finite element modeling approach is quantified, as this source of uncertainty has been acknowledged in the past as a potentially important factor to include in a seismic risk assessment (Aviram, Mackie, & Stojadinovic, 2008) yet there has been a lack of its systematic quantification particularly for RC buildings.

While fragility analyses based upon finite element simulation offer one important piece of a risk assessment to help characterize damage potential of the structure and its components, traditionally the term “risk” suggests incorporation of the consequences of damage (Ellingwood & Wen, 2005; Ghosh & Padgett, 2011). One important impact that damaged components have on post-earthquake performance is loss of functionality or business interruption attributed to the need for building closure and repair. Following an earthquake, tagging decisions are made based on the damage existing in a structure. These “tags” are brightly colored placards (red, yellow, and green) placed on the exterior of structures, which relate

to the usability and functionality of the building. They keep the public safe by informing passersby of the structure's current state and permissible occupancy. This information is presented both by the color of the tag and the content, which explains what was inspected, what structural issues were encountered, and who is allowed to enter. Damage in RC buildings has been observed and modeled, but for a proper assessment of the risk involved, i.e. safety concern for the public and structure damage, one needs to understand how the observed damage relates to closure or tagging decisions. Non-ductile RC buildings have a certain set of failures, as mentioned above, typically observed in post-earthquake reconnaissance. Liel (2008), Xue et al. (2009) and Hueste and Wight (1997) identify typical areas of damage and failure in reinforced concrete buildings. This thesis sets up a survey for professionals in the industry and academia to give their professional opinion of the condition of non-ductile RC buildings and state of safety for the occupants that coincide with tagging criteria that is adopted in states such as California, and also adopted in other countries outside of the US (Anagnostopoulos, Moretti, Panoutsopoulou, Panagiotopoulou, & Thoma, 2004; 1989; CPAMI, NAA, CUPCEA, CUPSEA, & PGEA, 2005). Therefore this thesis considers typical damage observed in non-ductile RC buildings, and first predicts the conditional probability of achieving those component failures based on finite element analyses and then constructs a survey to explore the likelihood of closure, cost, and repair strategies associated with the component damages. For future research the resulting models may be directly linked in order to more fully understand the risks associated with non-ductile RC building components or the benefits of alternative retrofits.

1.2. Organization of Thesis

This thesis is broken up into five chapters. Chapter 2 provides a literature review that focuses on past earthquake reconnaissance data for reinforced concrete buildings, various modeling techniques that have been used in seismic risk assessments, uncertainties that have been recognized for fragility analyses of RC buildings, and probabilistic risk assessment. Chapter 3 provides details on finite element modeling approaches to capture the response of non-ductile RC buildings and quantifies the uncertainty that may be associated with alternative modeling choices while also developing fragility curves for components in a reinforced concrete building. Chapter 4 discusses an online survey given to industry and academic engineering professionals to gather post-earthquake tagging decisions based on damages in reinforced concrete buildings and presents the analysis of the survey results. Chapter 5 concludes the thesis by discussing final conclusions from the data presented in the thesis while also discussing future recommendations to enhance the research.

Chapter 2

Literature Review

2.1. Reinforced Concrete Buildings in Seismic Regions

2.1.1. Inventory of Non-Ductile Reinforced Concrete Buildings

Non-ductile reinforced concrete (RC) buildings in areas of seismic activity are at great risk of minor to catastrophic damages at times of earthquake events. A recent Concrete Coalition report (Comartin et al., 2011) performed an inventory study of the existing RC buildings designed prior to the 1980s, finding that an estimated 17,000 buildings located in high seismic zones in California are still being used daily as private buildings, schools, and government offices. Prior to the 1980s, reinforced concrete design codes lacked the sufficient detailing needed for lateral seismic loads (Liel, 2008). Furthermore, in the Central and Eastern United States (CEUS), pre-1990 design procedures for RC frames typically accounted for gravity load design (GLD) only and neglected the seismic detailing needed. This later adoption of seismic design considerations in the CEUS has been attributed in part to the low frequency of observed

strong earthquakes and the additional costs associated with seismic detailing. Despite the subsequent code evolution and improvements in seismic design, many RC buildings built in past decades across the US are at risk of damage from earthquake activity.

2.1.2. Deficiencies in Non-Ductile Detailing

In contrast to seismically designed structures using modern codes, non-ductile RC structures are often characterized as having several distinct deficiencies. These deficiencies are the driving factors behind damages observed in post-earthquake inspections of non-ductile RC buildings. Inefficiencies with non-ductile design typically include: a) weak column-strong beam behavior; b) inadequate length of lap splices in the columns; c) inadequate amount of transverse steel located at column plastic hinge zones; d) inadequate amount of transverse steel in beam-column joints; e) discontinuity and short embedment length of bottom steel reinforcement in beams connected to the joints (Aycardi, Mander, & Reinhorn, 1994). Past earthquake events resulting in widespread damage have provided researchers and professionals with identifiable localized damage in non-ductile RC structures.

2.1.3. Typical Damage Observed in Reinforced Concrete Elements

The inefficiencies that are evident in non-ductile RC buildings as mentioned in the previous section directly influence the type of localized damages observed in post-earthquake reconnaissance. Common localized damage observed includes (Liel, 2008): 1) spalling of unconfined concrete; 2) flexural hinging in columns; 3) column shear failure; 4) flexure-shear failure in columns contributing to leaning or soft-story collapse of the structure; 5) joint shear concrete cracking and bar buckling; 6) longitudinal bar pullout. All of these observed damages correlate well with the deficiencies observed in

structures with non-ductile detailing. For example, the damage of flexural hinging in columns may be attributed to (a), (b), and/or (c) of the deficiencies previously stated. Knowing when a building was designed may be a key factor in determining the type of damage that may occur in seismic regions. Buildings designed prior to seismic design codes being introduced may be susceptible to the type of damages mentioned in (1)-(6). These susceptible elements in RC buildings have also been identified in tagging guidelines adopted in the United States and around the world.

2.2. Non-Linear Finite Element Modeling

Given the specific deficiencies of non-ductile RC buildings, significant research has been undertaken to model and predict the performance of such structures under seismic loading. Ranges of numerical modeling (i.e. Finite Element Modeling) programs, such as Opensees (McKenna, Mazzoni, Scott, Fenves, & al., 2006), SAP2000 (Computers & Structures, 2013b), and ETABS (Computers & Structures, 2013a), and procedures have been developed and adopted in research and practice to assess the vulnerability of RC buildings subjected to earthquake excitations. Since such a vulnerability evaluation requires understanding of the nonlinear response of the structure, modeling the post-elastic behavior of structural components for dynamic analysis of RC buildings has been largely investigated. Based on the level of knowledge required in the structural response, the configuration and the accuracy of the model may differ case to case.

2.2.1. Beam and Column Element Modeling

In some studies, beams and columns are modeled by using simplified lumped plasticity elements (Ibarra, Medina, & Krawinkler, 2005; Liel, 2008); while others define

fiber sections along the structural elements (Celik, 2007; Mitropoulou, Lagaros, & Papadrakakis, 2011). The fiber based models are characterized by a higher accuracy, but also by a higher level of complexity and of computational effort required. Another way to add accurate depictions of the responses to the FEM is through spring models located at areas of intense demand during seismic analyses. Spring models have been introduced to model the behavior of columns in shear and axial behavior (Elwood, 2004). These springs added at particular locations in the system allow the developer (of the model) to capture a more realistic demand from the component that may be defined by characteristics of the columns, beams, or joints. Another important difference can be attributed in the definition of beam-column joint behavior.

2.2.2. Joint Research

The definition of beam-column joint behavior in FEMs is crucial in the outcome of the analyses. In some cases rigid beam-column joint connections are adopted, either choosing to neglect the contribution of joint deformability in the model or using approximation methods to calculate joint demands (Celik, 2007; Mitropoulou et al., 2011). Otherwise past studies have investigated the use of different spring configurations to capture refined joint responses (Alath & Kunnath, 1995; Altoontash, 2004; Celik, 2007; Liel, 2008; Lowes, Mitra, & Altoontash, 2004). Springs are yet again adopted in order to capture a more realistic and accurate response of the component being studied in FEM analyses.

2.2.3. Uncertainties Associated with Seismic Analysis

Studies of alternative FEM strategies have typically focused on the comparison of models for an individual component within an RC building (e.g. alternative joint

models)(Alath & Kunnath, 1995; Altoontash, 2004; Elwood, 2004; Lowes et al., 2004). Moreover, in most of the cases, the comparison is based on evaluation of the deterministic behavior rather than by evaluating the seismic response given record-to-record variation among other potential sources of uncertainty. Proper assessment of the seismic vulnerability of structural systems should take into account all pertinent sources of aleatoric and epistemic uncertainties, including uncertainties in the seismic input (record-to-record variability), the properties defining the structural model (model parameter uncertainty) and the parameters defining the structure or components limit states (capacity uncertainty). The effects of input and capacity uncertainties have been largely investigated in past studies (Cornell, Jalayer, Hamburger, & Foutch, 2002; Vamvatsikos & Allin Cornell, 2002). Other researchers have recognized the importance of modeling uncertainties that affect the structural performance of numerical models, including the uncertainties in material and geometric properties and developed methodologies to evaluate their effect on the seismic response (Liel, Haselton, Deierlein, & Baker, 2009; Padgett & DesRoches, 2007; Tubaldi, Barbato, & Dall'Asta, 2012; Vamvatsikos & Fragiadakis, 2010). However, minimal research has focused on the uncertainty that exists between similar outputs collected using a variation of different modeling techniques to assess the seismic vulnerability of structures. Aviram et al. (2008) discussed the process of finding an epistemic uncertainty arriving from the use of two different modeling programs gathering the same responses in an identical structure. While Aviram acknowledged the idea and need for this epistemic uncertainty, the gap in his study arises from the lack of depth in the amount of data he gathers from various models to fully develop an uncertainty value. This source of uncertainty is becoming increasingly important to explore since, in

recent years, a multitude of modeling techniques have been developed and combined into FEMs for response and vulnerability assessment. Chapter 3 builds upon this minimally introduced uncertainty parameter accounting for the dispersions that arise from the wide variety of possible FEM modeling techniques. This uncertainty parameter should be introduced in the probabilistic assessment of structures in order to derive results independently from the modeling techniques used. No perfect model exists to assess the seismic vulnerability of RC buildings, so an uncertainty parameter is needed in the probabilistic assessment framework that acknowledges the uncertainty that exists between the various modeling techniques used in research and practice.

2.3. Probabilistic Risk Assessment of Reinforced Concrete Buildings

Cornell et al (2002) introduced the basis of the probabilistic framework that is used in this thesis for vulnerability assessment of structures. Their studies concluded that a power model best described the behavior between an engineering demand parameter (EDP) and an intensity measure (IM). By transforming the demands and IMs in the log-log space, a linear relationship exists. This relationship typically holds true for global EDPs such as drift, acceleration, and velocities, but a more refined relationship in the log-log space is needed for local EDPs. The local EDPs, such as strains in concrete and steel, shears, and moments, are best described using a bilinear relationship in the log-log space. Described by Bai et al. (2011) and Ramamoorthy et al. (2006), the bilinear regression models more accurately capture the relationship between EDPs and IMs.

A probabilistic risk assessment is important in understanding the possible consequences of a non-ductile RC being damaged during an earthquake (Ellingwood, 2001; Tesfamariam & Saatcioglu, 2008). While risk is sometimes described as probability of failure of components or the building as a whole (Ellingwood & Wen, 2005), there are other risks that evolve from the consequences of damage (Kinali & Ellingwood, 2007; Padgett & DesRoches, 2007; Wen & Ellingwood, 2005). Once a structure is damaged, there are inherent risks to the public, building owners and occupants, and adjacent structures. These type of risks are typically assessed during a rapid evaluation of structures following an earthquake event. The tagging of buildings represents the risks posed to the public and nearby infrastructure.

2.4. Tagging Guidelines for Reinforced Concrete Buildings

Tagging guidelines and procedures presented in papers and reports from around the world identify critical zones in a structure that may exhibit damage after an earthquake (Anagnostopoulos et al., 2004; 1989; CPAMI et al., 2005). Models that simulate and capture demands, correlating with reported typical damage, are often used in the risk assessment of RC buildings (Alath & Kunnath, 1995; Celik, 2007; Elwood, 2004; Liel, 2008). Subsequently, repair and loss estimation models are important tools that are coupled with the damage models to predict the costs of damage to a building or components within a building (Bal, Crowley, Pinho, & Gülay, 2008; Goulet et al., 2007; Kircher, Nassar, Kustu, & Holmes, 1997; Xue et al., 2009). Models of anticipated post-event tagging decisions are also important because these decisions affect the prospective use of the structure and potentially indirect losses associated with building use and occupancy. They may also correlate to anticipated repair

durations and costs. Furthermore, when integrated in a performance-based assessment, the likelihood of a tag may also serve as a potential factor for risk-informed decision making on investment in level of design or retrofit. To develop a tagging criteria based risk assessment, others have followed a “prescriptive” approach that defines what tag a building should be given based upon a suggested limit state for the damage type (Maffei, Telleen, & Nakayama, 2008; Xue et al., 2009). Such approaches are valuable for offering guidance on recommended tagging procedures such that an assigned tag aligns with a given set of building performance criteria. However, this study takes a “subjective” approach, recognizing that variation exists in expert opinion regarding tagging of buildings and that the outcome is uncertain. The variation mentioned is captured through a survey that aims to provide insight into the likely tag assigned based upon visual damage observed, along with supplemental information on potential repairs.

Comparison of Modeling Strategies to Capture Component Level Damage in Non-ductile Reinforced Concrete Buildings

3.1. Introduction

This chapter will address gaps evident in the numerical modeling and probabilistic assessment of non-ductile RC buildings as mentioned in section 2.2. There are many ways to create finite element models (FEMs). As mentioned in chapter 2, past studies have developed component level models to more accurately predict the response of analytical models. The choices available for researchers to implement in final FEMs for their respective studies are abundant. The gap in research involves the uncertainty arising from using various modeling approaches that may exist to represent the same design. The gaps are addressed by comparing alternative levels of modeling fidelity for non-ductile RC buildings. First their ability to reproduce experimental test

data is compared, and subsequently their influence on the probabilistic seismic response evaluation is investigated. Component level responses are emphasized in addition to global responses to highlight the influence of alternative models on probabilistic estimates of local EDPs of interest for next generation damage, functionality, and loss assessment. Four different modeled building combinations are considered. The more sophisticated model includes a joint model (Alath & Kunnath, 1995) able to capture the joint deformability and a shear-axial model (Elwood, 2004) able to reproduce the shear failure. The simpler model uses rigid connections between the beams and columns. The deterministic behaviors of the models are compared by observing global as well as local level EDPs. Moreover, the probabilistic behavior of these response parameters for each model is investigated performing a probabilistic seismic demand analysis (PSDA) (Shome, 1999) and conducting a t-test (Neter, Kutner, Nachtsheim, & Wasserman, 1996) for statistical comparison of the resulting models. Finally, a new FEM uncertainty parameter to be used in future vulnerability analyses is developed from dispersion data between the different models.

3.2. Alternative Modeling Approaches

In this chapter a case study structure is adopted to test the influence of alternative modeling strategies, including comparison and validation with past experimental test data of the structure as well as quantification of model influence on probabilistic response assessment at the local and global levels. The case study adopted, including its range of relevance, and the details on the numerical modeling approaches are presented in the following subsections.

3.2.1. Case Study Structure

The case study structure adopted is representative of RC buildings typically designed prior to the adoption of modern seismic codes and seismic detailing in the CEUS. Past studies in California (Comartin et al., 2011; Liel, 2008) suggest that low-rise buildings ranging from 1 to 3 stories dominate the inventory, while the bay widths of typical RC frames span from 5.5 to 9.2 m. El-Attar et al. (1991) determined that typical non-ductile RC buildings located in the CEUS have 3.6 meter story heights with bay widths spanning from 4.9 to 9.2 m. Hence, although the investigation conducted in this study focuses on a single structure, the case study is selected to be representative of typical non-ductile RC buildings across the US while also offering an opportunity for model validation with experimental data. However, further studies are needed to confidently generalize the results for different geometries.

The case study structure, as seen in Figure 3.1, used in this investigation was experimentally tested by Bracci et al. (Bracci, Reinhorn, & Mander, 1992a). A typical RC office building found in the CEUS was designed for gravity load only by following ACI 318-89. The RC building has 3 stories at individual heights of 3.66 m with 3 bays at widths of 5.49 m each. The material properties specified for the buildings are ASTM 615 Grade 40 steel ($f_y = 275$ MPa) and ordinary Portland cement concrete at a 28-day compressive strength of 24 MPa. Cross-section details for the columns and beams, as well as distributed loads applied to the structure, are reported in Bracci et al. (1992a). The distributed dead and live loads applied to the case study structure are 5.2 kN/m² and 2.4kN/m², respectively. All the models developed in this study follow the same general specifications stated herein to satisfy the typical case study structure.

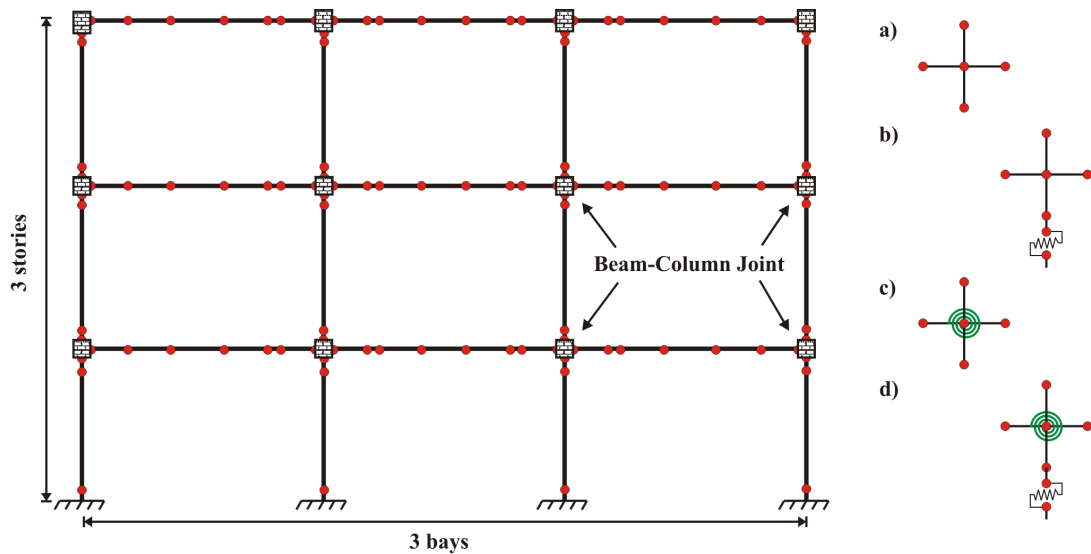


Figure 3.1 - OpenSees full-scale two-dimensional model with four different combinations of the joint and column spring details: a) rigid, b) column, c) joint, d) joint-column. Beam and column section detailing is referenced (Bracci et al. 1992a).

The open-source computational framework OpenSees (McKenna et al., 2006) is adopted to perform nonlinear dynamic analyses. Four different modeled building combinations are considered. The first model is termed as: 1) *rigid model* employing *force based beam-column elements* (McKenna et al., 2006) with fiber discretized cross-sections in order to represent the beams and columns, rigid elements at the joints, and neglects shear deformations. The other models are upgrading from the *rigid model* by employing local models to represent the shear and axial behavior of columns, behavior of joints and the behavior of both these components together. Hereinafter they are referred to as: 2) *column model*, 3) *joint model* and 4) *joint-column model* and are described in the following sections.

The hysteretic behavior of concrete is modeled with *Concrete02* uniaxial material model (McKenna et al., 2006), and the ratio of unloading to loading slope used in this study is equal to 0.1. The concrete material properties are defined based on experimental data of the one-third scale model constructed by Bracci et al. (1992a).

The properties of the confined concrete have been evaluated by using the formulation proposed by Mander et al. (1988) and have been applied to the fibers of the core section. However the effect of the confinement has been found to be minimal given the limited transverse reinforcement provided in the structure. The behavior of steel reinforcement is described by the *Hysteretic* uniaxial material model (McKenna et al., 2006). Steel yield strength is increased by 25% from the nominal value of the ASTM 615 Grade 40 steel to account for material overstrength as suggested by Aslani and Miranda (2005). Damping sources other than the hysteretic dissipation energy are modeled by Rayleigh damping, with mass and stiffness coefficients calibrated such that 3% damping is obtained for the first two vibration modes.

3.2.2. Rigid Model

In the *rigid model*, the joints are modeled by connecting the adjacent beam and column nodes with idealized perfectly rigid beam-column elements. These rigid links serve to reflect the physical dimension of the joint and allow moments and forces to be fully transmitted through the joint to the surrounding elements. As noted by Celik (2007), potential limitations of such models include their inability to respond to the actual joint panel deformability observed in real structures. Moreover, the joint panel shear has been observed as a critical section of failure in RC buildings (Priestley, 1997).

3.2.3. Column Model

The *rigid model* is upgraded into the *column model* by including the column shear-axial model developed by Elwood and Moehle (2008). Given that RC columns are susceptible to flexure-shear failure in earthquake events, Elwood and Moehle (2008) developed the *LimitState* uniaxial material model (McKenna et al., 2006) based on a

hysteretic uniaxial material. This material model is applied to zero length springs along the column permitting characterization of the local shear behavior of columns. The *LimitState* material updates the column response curve once a shear force and axial force limit have been reached. The limits to be reached are defined using a shear limit curve and axial limit curve, which are defined based upon parameters that depend upon the column detailing and orientation used in the case study building. The structure specific parameters integrated in the model include concrete compressive strength, column width, column depth, effective column depth, and transverse reinforcement ratio. Furthermore, the *LimitState* material requires OpenSees specific parameters to define the backbone of the axial and shear curves. These parameters are summarized in Appendix A, Table A.1. The use of this local model permits the FEM to account for the instance of shear failure and loss of axial load carrying capacity in the column.

3.2.4. Joint Model

The *rigid model* is upgraded into the *joint model* by including the joint model developed by Alath and Kunnath (1995) and investigated by Celik (2007). Celik (2007) compared four different types of joint models finding that the scissors model with rigid end zones (Alath & Kunnath, 1995) best predicted the response of experimentally tested subassemblages by coupling accuracy of the results and the relative simplicity of the rotational spring model for representing joint behavior. This model is therefore adopted in this study.

The scissors model is implemented in OpenSees by employing the *Pinching4* uniaxial material model (McKenna et al., 2006). In particular, it is used to describe the rotational behavior of a zero length spring placed at the joint connection, following the

procedure described in further detail in Celik (2007). The *Pinching4* material allows the definition of a multi-linear backbone curve, along with pinched response and strength degradation from unloading and reloading. The moment-curvature backbone is defined based upon cracking, yielding of reinforcement, joint shear strength, and residual strength, where the latter three are identified from a static pushover analysis. The initial joint shear cracking stress is defined by ACI (ACI-ASCE, 1976), where the shear stress is estimated as

$$\tau_{cr} = 3.5 * \sqrt{f'_c (1 + 0.002 * (N_u / A_g))} \quad (\text{psi})$$

Equation 3.1- Joint shear cracking stress

where f'_c is the 28-day concrete compressive strength (psi) in the joint, N_u is the axial load (lbs) applied through the joint, and A_g is the gross cross-sectional area (in²) of the joint perpendicular to the axial load direction. Table A.2, in Appendix A, defines the unloading and pinching parameters for the *Pinching4* material.

By incorporating the joint models, the structural model is able to capture the joint panel deformation and degradation of strength during the seismic excitation. The *joint-column model* utilizes both the aforementioned column shear-axial and joint springs within the same finite element model of the case study building.

3.3. Model Comparisons with Experimental Data

The models described above are compared with available experimental data to gain insight into their relative performance and their ability to reproduce observed behaviors. Interior and exterior joint subassemblages have been modeled to investigate

the importance of the different modeling strategies on their lateral load cyclic behavior. The results of the models are compared with the experimental results from Aycardi et al. (1994). Moreover, the global and local response of the models under dynamic excitation are compared with the available experimental results from Bracci et al. (1992b). The findings are discussed in the following sections.

3.3.1. Subassemblage Model

Aycardi et al. (1994) constructed one-third scale models of interior and exterior subassemblages in order to investigate the experimental response of joints with non-seismic detailing. The subassemblage dimensional specifications and material properties were adopted from the one-third scale 3-story by 3-bay RC frame developed by Bracci et al. (1992a and 1992b). The interior and exterior subassemblages were axially loaded and subjected to reversed cyclic lateral displacements of increasing drifts until failure. In this study, the interior and exterior joints are modeled in OpenSees as described above and compared to the lateral load-drift experimental results. Only the *rigid* and *joint* models were used for comparison with experimental results. The *column model* is not considered for this comparison since the assembly of the joint subassemblage created by Aycardi et al. (1994) does not capture the complete affect of an entire column experiencing shear degradation, and consequently the failure condition observed by Elwood and Moehle (2008).

Figure 3.2 and Figure 3.3 show the comparisons between the experimental data and the results carried out by the *rigid* and *joint* models respectively for the interior and exterior subassemblages. From the interior subassemblage comparison (Fig. 3.2), it can be observed that the *joint model* captures the degradation and pinching behavior more

accurately as compared to the *rigid model*. While the *rigid model* response compares well with the experimental response in the negative drift range, the response in the positive drift range accounts for only about two-thirds of the experimental lateral load as the subassemblage continues to yield. Despite the improvement in capturing degradation and pinching, the *joint model* under-predicts lateral load in the positive drift range while over-predicting by twenty percent in the negative drift range. Aycardi et al. (1994) similarly tried to simulate the behavior of the subassemblage with FEM and also saw such relative over- and under-predictions. They attributed these observations to the lack of consideration of bond deterioration in the model. Referring to the exterior joint subassemblage comparisons (Fig. 3.4), the ability to capture degradation and pinching behavior is still noticeably better in the *joint model*. For the comparison in the exterior subassemblage, the *joint model* more accurately predicts the lateral load response in the inelastic range. In terms of deviations in peak lateral load at each cycle from the analysis relative to the experiment, the *joint model* shows an average of 5% improvement in predictive abilities when compared to the *rigid model* for both the interior and exterior joint. As a result of the validation comparisons, it is observed that the *joint model* is better able to reflect the local component behavior, as intended in its development, and instills greater confidence in the model. However, the relative impacts of differences in adopting the modeling strategies within a full building or for probabilistic performance assessment are yet to be explored.

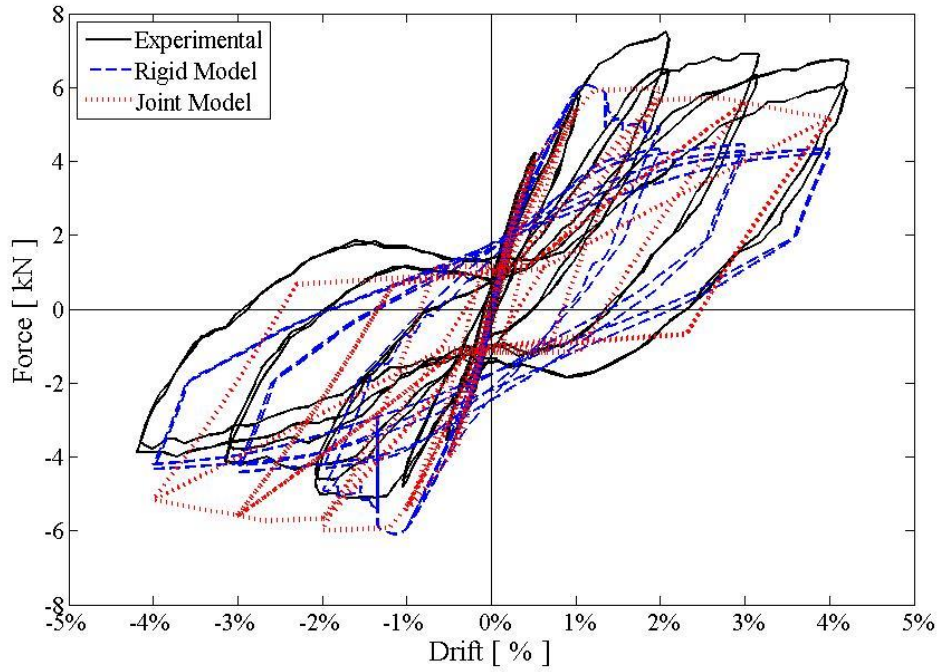


Figure 3.2 - Comparison of the rigid and joint models to experimental data for the interior subassembly.

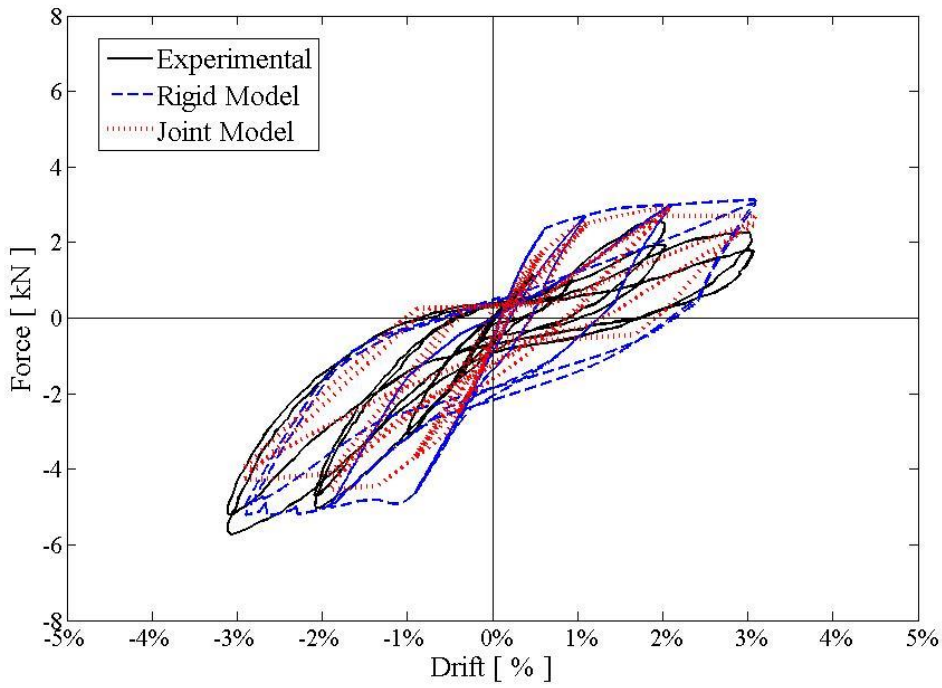


Figure 3.3 - Comparison of the rigid and joint models to experimental data for the exterior subassembly.

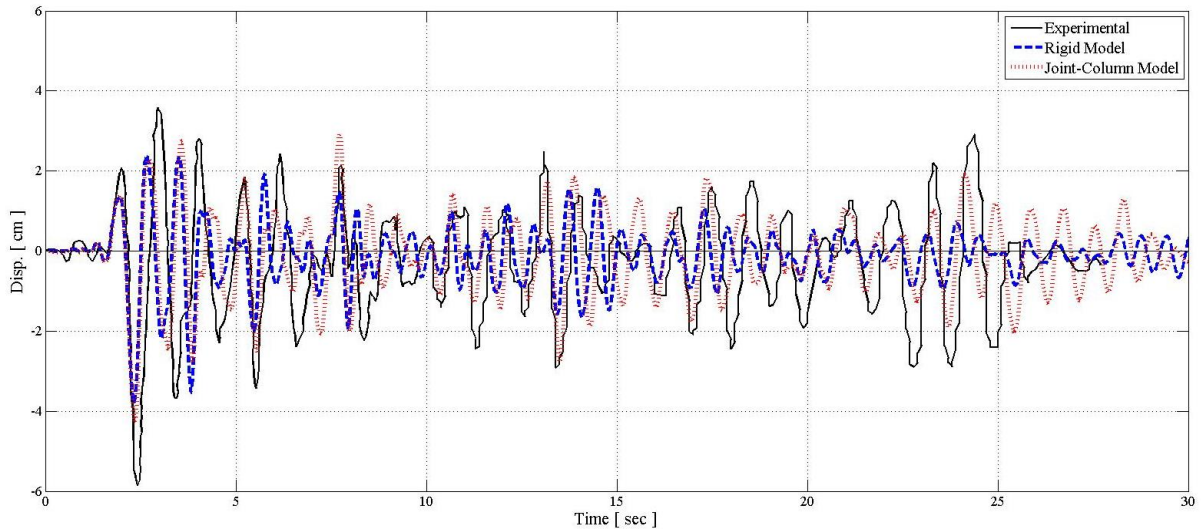


Figure 3.4 - 3rd story displacement data for comparing one-third experimental with rigid and joint-column models using dynamic analysis ground motion from Taft at PGA of 0.30g.

3.3.2. One-third Scale Model

Bracci et al. (1992a and 1992b) experimentally tested a one-third scale model of a 3-story by 3-bay RC frame. The experimental model was subjected to shaking table tests of the Kern County 1952, Taft Lincoln School Station, N021E component record scaled to three different values of peak ground acceleration (PGA): 0.05g; 0.20g; 0.30g. Table 3.1 presents a comparison of the natural vibration periods and modal shapes from the finite element models and those derived from the experiment. White noise tests were applied before and after each ground motion record to obtain estimates of the periods and mode shapes of the damaged building in the experiment. The dynamic characteristics of the experimental model, determined from the white noise tests conducted after the scaled ground motion intensities, are stated in Table 3.1 to compare with the numerical models' dynamic characteristics. The mode shapes are relatively consistent between the models and experiment, whereas some differences exist in the estimates of the periods. During the 0.20g PGA motion the experimental model first

yields and begins an inelastic response for the duration of the experiment. The natural periods determined beyond the yielding of the scaled experimental building provide a closer relationship with the natural periods determined from the nonlinear FEM analyses.

Table 3.1 - Dynamic characteristics of experimental vs. analytical modeling techniques; period values in parentheses are the natural periods observed in the experimental model after the Taft 0.05g, 0.20g, and 0.30g PGA ground motions.

Model	Natural Periods (s)	Mode Shapes		
<i>Experimental</i>	0.97 (1.01) (1.22) (1.44)	1.00	-0.82	-0.46
	0.33 (0.34) (0.40) (0.46)	0.80	0.46	1.00
	0.22 (0.23) (0.28) (0.33)	0.42	1.00	-0.83
<i>Rigid / Column</i>	1.30	1.00	-0.81	-0.44
	0.45	0.79	0.50	1.00
	0.30	0.41	1.00	-0.85
<i>Joint-column / Joint</i>	1.34	1.00	-0.81	-0.43
	0.46	0.78	0.52	1.00
	0.30	0.40	1.00	-0.87

Comparisons in the dynamic responses were made for all levels of ground motion between the experimental data and numerical models developed. The third story displacement time history for the 0.30g PGA motion is shown in Figure 3.4, showing the comparison between the experimental, the *rigid model* and *joint-column model* responses. The *column model* response is equal to that of the *rigid model* while the *joint model* response is equal to that of the *joint-column model* since shear and axial failure was not observed during the analysis, consistently with the experimental test observations. The results also show that there is some deviation in the amplitude of responses throughout the time history, but that the frequency of response is fairly consistent. Furthermore, the peak values of floor displacements are well captured by both models for all levels of ground motion considered, which is of primary interest in

most probabilistic seismic response analyses and reliability studies. As shown in Figure 4, the maximum third story displacement captured by the numerical *rigid* and the *joint-column model* are respectively 31% and 20% smaller than the experimental results. This suggests that the *joint-column model* has a slight advantage in capturing global responses, which is attributed to its ability to capture joint deformations. The smaller ground motions of 0.05g and 0.20g PGA also exemplify this trend of a slight advantage in capturing global responses. The 0.05g PGA Taft ground motion captured errors of 5% and 16%, respectively, for the *rigid* and *joint-column models*. The 0.20g PGA errors are 21% and 31% for the *rigid* and *joint-column models*.

The results of the comparison with experimental test data suggest that overall the numerical models perform well in capturing component level and global behavior, forming a solid basis for utilization of the models in a probabilistic performance assessment that explores alternative levels of ground motion and inferences regarding form of predictive demand models. They also suggest that the *joint* or *joint-column model*, as the most rigorous modeling techniques, can provide more accurate estimates of local and global behavior and hence serve as a benchmark comparison in the probabilistic analysis. The experimental data for the case study building does not enable explicit validation of the *column model*, given that such failures were not observed in the tests and logically not predicted in the simulations. The component level column model validation was conducted by the developers Elwood and Moehle (2008).

3.4. Impact of Modeling Approach on Probabilistic Seismic Response Assessment

Nonlinear dynamic analyses were performed on the four numerical models described, gathering EDPs in order to make comparisons between local and global demands of the simulated models. Probabilistic seismic demand models (PSDMs) are captured from the EDPs output from the simulations run from the four FEMs. The t-test (Neter et al., 1996) was utilized as an assessment for the PSDM data collected, providing a statistical test of the difference between probabilistic seismic demand models predicted using data from alternative FEMs. An uncertainty value is defined based upon the differences observed between output from the four numerical models. These methods chosen to test the variations in the data provide insight into the discrepancies seen when using variations of modeling techniques.

3.4.1. Probabilistic Seismic Demand Analysis of System and Components

Probabilistic seismic demand analyses (PSDAs) were performed by subjecting each FEM to a suite of 220 ground motions. One hundred ground motions were taken from a suite identified by Krawinkler et al. (2003) and 120 from Baker et al. (2011). These two suites were utilized in order to gather data from a wide spectrum of earthquake characteristics. The types of EDPs gathered from the analysis and used for the probabilistic analyses are presented in Table 3.2. The 10 EDPs are defined in terms of local and global characteristics of the building under earthquake loads and for each analysis they are the maximum-over-time values of the demand. Global EDPs are widely employed since they synthetically describe the structural demand and permit to estimate the overall damage of structures and to provide insight into the damage of

buildings' non-structural components and contents. The local EDPs chosen are linked to localized component damages observed in RC buildings after earthquake events, mentioned in section 2.1, and provide sufficient data to make quality comparisons accounting for the effect of the incorporated local models.

Table 3.2 - Local and global engineering demand parameters considered for probabilistic seismic demand models.

EDP	Description	Failure Type
Global		
θ_i	Interstory drift	Structural and Non-Structural
St. Acc. _i	Story acceleration	Contents and Non-Structural
Local		
$\epsilon_{c \text{ col}}$	Column concrete strain at extreme fiber	Flexural and Axial
$\epsilon_{s \text{ col}}$	Max column steel strain	Flexural and Axial
$\epsilon_{c \text{ beam}}$	Beam concrete strain at extreme fiber	Flexural
$\epsilon_{s \text{ beam}}$	Beam steel strain	Flexural
V_{col}	Column shear	Shear Resistance
M_{col}	Column moment	Bending Resistance
$\epsilon_{j \text{ int}}$	Joint strain at interior joint	Joint Shear
$\epsilon_{j \text{ ext}}$	Joint strain at exterior joint	Joint Shear

A probabilistic seismic demand model (PSDM) is the outcome of the PSDA and it is the mathematical description of the relation between a seismic intensity measure (IM) and the EDP of interest. An IM defines the salient features of the ground motion that affect the structural response. Ideally, an IM should be able to capture the amplitude, frequency content and duration properties of ground motion that significantly affect the elastic and inelastic response of the system. The spectral displacement corresponding to the fundamental period of the structure $S_d(T_1)$ has been

chosen as IM for this investigation. Previous research demonstrated (Freddi et al., 2012) the adequacy of this IM to be employed while investigating the behavior of low-rise RC buildings.

3.4.1.1. Linear Regression Models

Cornell et al (2002) introduced the basis of the probabilistic framework that is used in this thesis for vulnerability assessment of structures. In their studies, they found that the relationship between median structural demand and intensity measure (IM) can be related to a power model given by:

$$Demand = aIM^b$$

Equation 3.2 - Demand power model developed by Cornell et al. (2002)

where a and b are regression coefficients. By transforming the output demands and IMs in the log-log space, the regression model may be characterized by a linear equation written in the following way:

$$\ln(Demand) = \ln(a) + b \ln(IM)$$

Equation 3.3 - Linear representation of the power model in the log-log space

The final parameter needed to fulfill the probabilistic framework is the dispersion about the median demand from the regression models. This dispersion, $\sigma_{D|IM}$, is computed from the data in the log-log space and may be seen as a logarithmic standard deviation. The $\sigma_{D|IM}$ is assumed to be homoscedastic along the entire demand median in the regression model. This homoscedastic approach may not be accurate in describing a particular demand in the probabilistic assessment.

3.4.1.2. Bilinear Regression Models

Bilinear regression models for probabilistic assessments were developed to describe two areas of different behavior when studying the demands of a particular finite element model (FEM). Many engineering demand parameters (EDPs) may respond in a nonlinear fashion in the log-log space given increasing IMs. While it is mostly acknowledged that global EDPs, i.e. drift and acceleration, follow a linear representation, many local EDPs, i.e. shear, moments, and strains, follow a non-linear characteristic as IMs increase (Freddi et al., 2012). Described by Bai et al. (2011) and Ramamoorthy et al. (2006), the bilinear regression models can be written as:

$$\ln(Demand_1) = \ln(a) + b \ln(IM)$$

Equation 3.4 - First linear regression in the bilinear model where $\ln(IM) \leq \ln(IM_{mid})$

$$\ln(Demand_2) = \ln(a) + b \ln(IM) + d[\ln(IM) - \ln(IM_{mid})]$$

Equation 3.5 - Second linear regression in the bilinear model where $\ln(IM) \geq \ln(IM_{mid})$

For the EDPs listed in Table 3.2, a bilinear regression model in the log-log space is needed to better describe the elastic and post-elastic behavior. Figure 3.5 illustrates the differences between linear and bilinear PSDMs using the global and local EDPs. In particular, the interstory drift at the first story and the moment of the interior column at the first floor are reported. All bilinear regression models include the linear regression line for comparison. These PSDMs are both outcomes of the *joint-column model*.

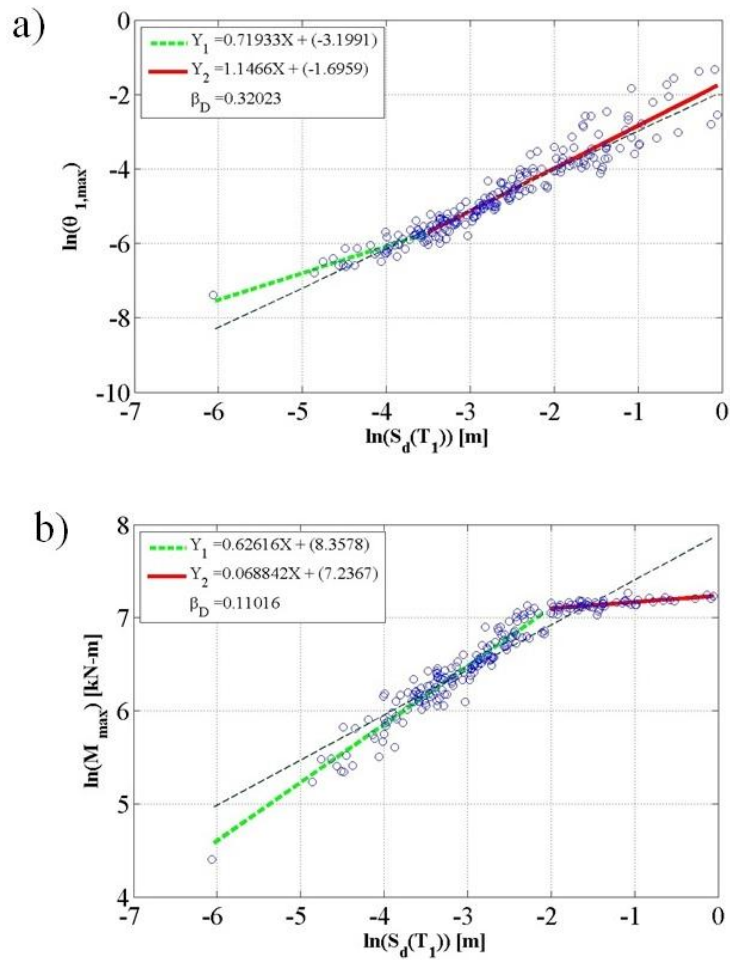
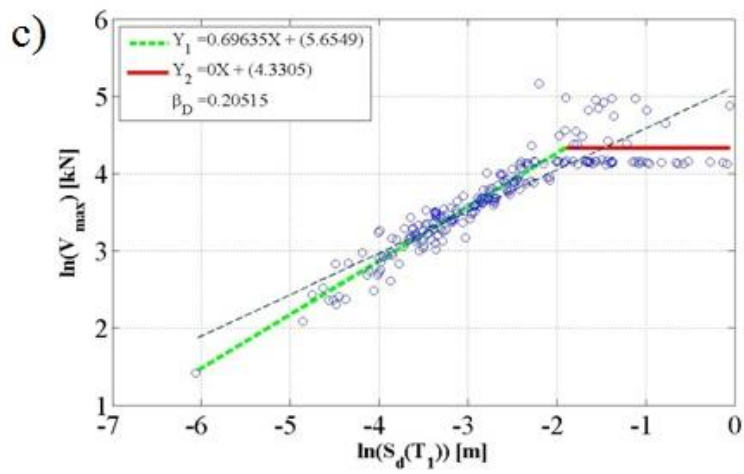
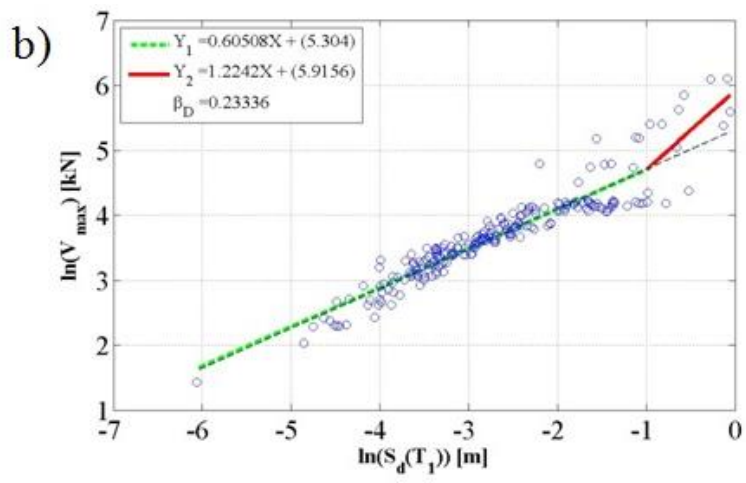
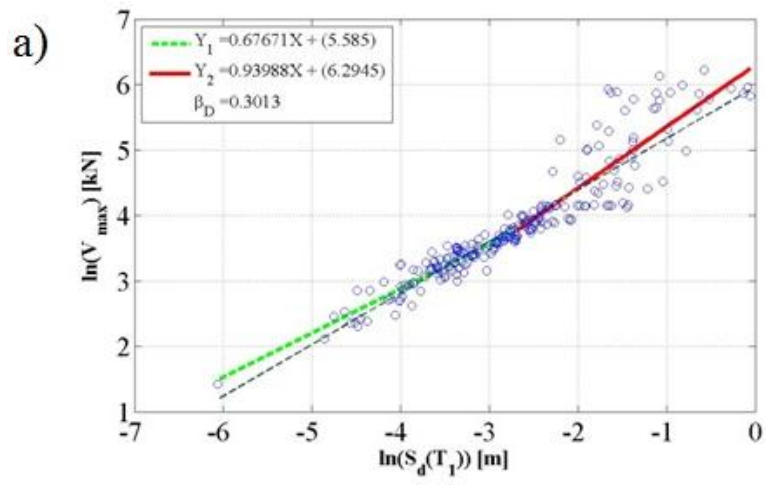


Figure 3.5 - Rigid model PSDM for: a) maximum interstory drift at first floor, seen as linear; b) maximum moment at the interior column on first floor, seen as bilinear. $S_d(T_1)$ is used as the IM.

Figure 3.6 shows the bilinear PSDMs for the shear of the interior column at the first floor for the four numerical models. It is noticeable that the *shear* and *joint-column models* are similar while the *rigid* and *joint* models differ from the models with an applied shear-axial model. Figure 3.7 illustrates the PSDMs of interior joint strain only attained from the *joint* and *joint-column models*. The *rigid* and *column models* do not gather demands located at the joint during simulations.



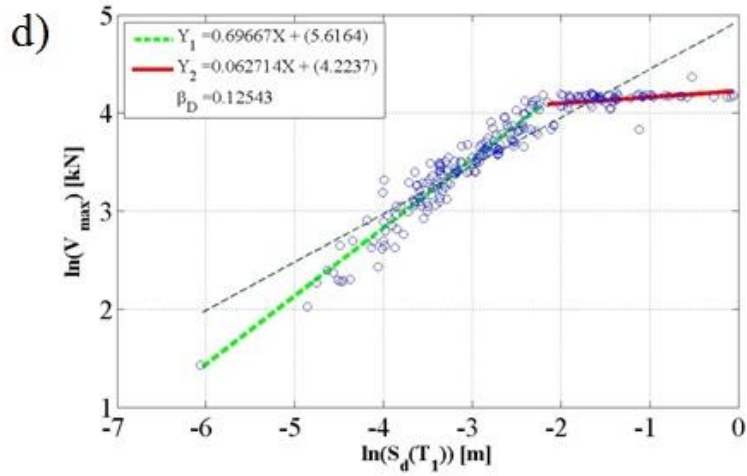


Figure 3.6 - Bilinear PSDM for maximum shear at the interior column on the first floor in: a) rigid b) joint c) column and d) joint-column models. $S_d(T_1)$ is used as the IM.

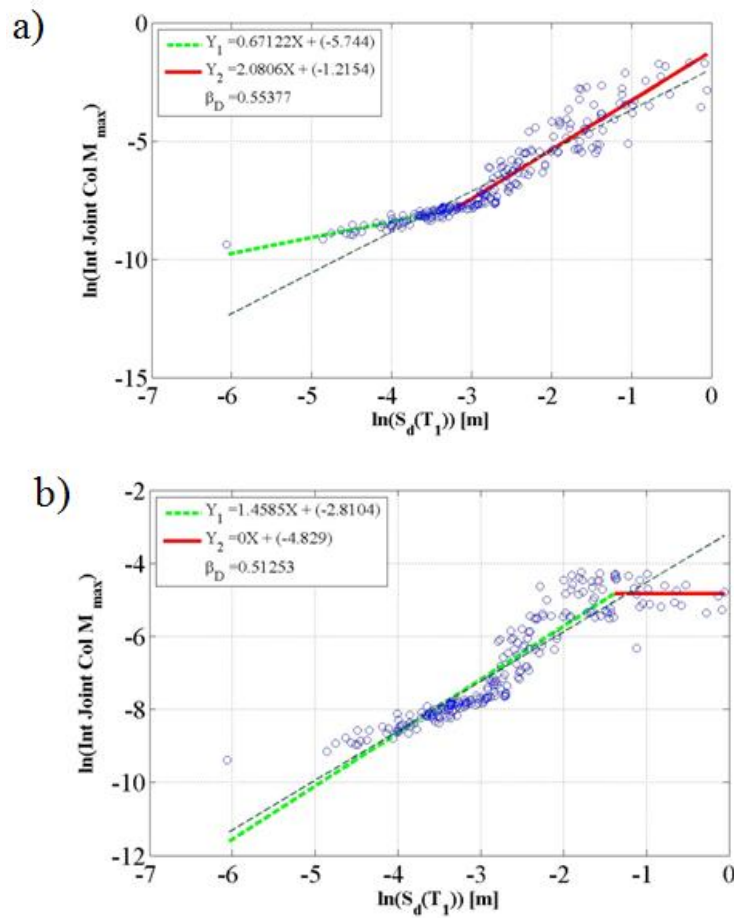


Figure 3.7 - Bilinear PSDM for maximum interior joint strain at the first floor in: a) joint and b) joint-column models. $S_d(T_1)$ is used as the IM.

3.4.2. PSDM Comparisons

The t-test (Neter et al., 1996) is employed herein to compare the PSDMs of the four numerical models in order to assess if there is a statistical difference between the median values of the regression data. The *joint-column model* is the model that better represents the real behavior of the structure, and hence, it is used as reference for which comparisons are conducted. The t-test offers a statistical hypothesis test and is used as a comparative tool between two linear regression lines to identify with a confidence level whether they are similar or not. In order to use the t-test within bilinear regressions, the test is performed for three parts of the bilinear PSDM where the comparisons are made between the first regression lines, between the overlap of the first and second regression lines, and between the second regression lines of the four finite element models. The second comparison occurs because of the unequal starting points of the second regression line.

Table 3.3 presents the results of each t-test. A value of 1 is reported if a statistical similarity exists with 90% confidence between the comparative models at the desired component level; a value of 0 is reported otherwise. The interstory drift and story acceleration of the third floor shown in Table 3.3 consider only the first line of regression since only linear PSDMs are used for global EDPs. From Table 3.3, the global EDP relationships are similar between the *column* and *joint-column model*, whereas the *rigid* and *joint models* do not exhibit similar median value behavior when compared to the *joint-column model*. This is depicted by a value of 0 indicating a statistically significant difference between the models. While examining local EDPs, there is more similarity between the *column* and *joint-column models* as compared to the other two comparisons. All comparisons show similarities in the first regression line comparisons,

whereas second regression line comparisons are only similar between the *column* and *joint-column models*. This is logical since both models employ the *column model* that defines a failure point in the simulations, whereas the models not including the *column model* continue their simulations until the end of the ground motion run. The amount of energy dissipated through deformations in each numerical model influence the resulting regression lines. For example, the implementation of the local joint model dissipates energy that would otherwise be distributed through the other structural elements around the joint. Differently, the numerical models incorporating the *column model* may fail to converge during the analysis of particular ground motions. Even though the model may fail to converge, the demand data is still gathered and used in the regression analysis at failure. Hence, including this local model influence the regression by not allowing exaggerated element deformations otherwise recorded. These adjusted slopes are evident in the comparison of the second regression lines between the four FEM models, as seen in Figure 3.6, which compares the shear EDP. A stronger relationship exists between the base *joint-column* and *column* model, but there are fewer relationships when comparing the *joint-column* to the *joint* and *rigid* models. The FEMs that do not incorporate the local column model express values beyond the building's actual shear capacity. The different relationships shown in Table 3.3 may be evidence for a FEM uncertainty to be examined between the four numerical models being compared.

Table 3.3 - T-test results comparing PSDM data from the four analytical models; (1) indicates existent relationship , whereas (0) indicates no relationship with 90 percent confidence.

Regression Line:	<i>Joint vs. Joint-Column</i>			<i>Column vs. Joint-Column</i>			<i>Rigid vs. Joint-Column</i>		
	1st	1st v. 2nd	2nd	1st	1st v. 2nd	2nd	1st	1st v. 2nd	2nd
θ_3	0	← Only linear consideration		1	← Only linear consideration		0	← Only linear consideration	
St. Acc. ₃	0			1			0		
$\epsilon_{c \text{ col}}$	0	0	0	1	0	1	0	0	0
$\epsilon_{s \text{ col}}$	0	1	0	1	0	1	0	1	0
$\epsilon_{c \text{ beam}}$	1	0	1	0	0	1	0	0	0
$\epsilon_{s \text{ beam}}$	1	0	1	0	0	0	1	0	0
V_{col}	1	0	0	1	0	0	1	0	0
M_{col}	1	0	0	1	0	1	1	0	0
$\epsilon_{j \text{ ext}}$	1	0	0	N/A			N/A		
$\epsilon_{j \text{ int}}$	0	0	0						

3.4.3. Finite Element Model Uncertainty

Many sources of uncertainty have been identified in the past including aleatoric record-to record variability (σ_D) (Cornell et al., 2002), epistemic modeling uncertainty (σ_M) (Liel et al., 2009), and the epistemic capacity uncertainty associated with each limit state (σ_c). The record-to-record variability and the modeling uncertainty lead to dispersion in the demand. The first parameter is a consequence of the randomness of the seismic excitation properties; the second parameter accounts for the lack of knowledge in terms of material property, geometric configuration, floor mass, damping properties and other properties concerning the structure analyzed. The capacity uncertainty is usually defined by experimental tests for various performance levels.

The differences observed among the 4 model combinations considered in this study highlighted the need to introduce, amongst others, an additional uncertainty parameter, σ_{FEM} , accounting for the variation of demand from the wide variety of possible FEM modeling techniques. In particular, many researchers have made conclusions (e.g. fragility estimates, damage risk curves, or even economic loss estimations) based on their respective models created as FEMs. There does not seem to be a universal choice of modeling approach and hence accounting for the finite element model uncertainty permits a basis of comparing results carried using different modeling techniques.

The σ_{FEM} is directly calculated from the variation in the log-log space between demand outputs of two different modeling combinations and considering the EDPs listed in Table 3.2. For a given IM value defined from the ground motions used in the analyses, the variation is calculated as:

$$\Delta_i(j,k) = \ln(\text{EDP}_j) - \ln(\text{EDP}_k)$$

Equation 3.6 - Variation of demands between various finite element models

where $\Delta_i(j,k)$ is the variation of the demand of the i^{th} EDP from Table 3.2; EDP_j and EDP_k are the demands of j and k models: *rigid*, *joint*, *column*, and *joint-column*. Figure 3.8 shows the variation of one EDP in a scatter plot with respect to the IM value. The EDP used in Figure 3.8 is the shear located at the interior column of the first story. As seen in Figure 3.8, the dispersion of the data grows larger past $\ln(S_d(T_1)) = -2.5$. Similar results can be observed by looking at other EDPs and other components. As consequence of this different behavior of

the variation of demand depending upon the value of IM, the dispersion is calculated independently for two sets of samples divided by the value of $\ln(S_d(T_1)) = -2.5$. Table 3.4 presents the standard deviations for each set of data already transformed in the log space, as seen in Figure 3.8. These values provide an estimate of the dispersion attributed to demand variation resulting from FEM approaches. The σ_{FEM} values representing the lower range of IMs are small; this occurs since the upgrading of the *rigid* model are mostly introduced in order to model the post elastic behavior of the structure. In the higher range of IMs, the σ_{FEM} values for the local EDPs of column concrete strain (1.45), interior joint strain (1.24), and exterior joint strain (1.22) are significantly larger than the other values. Since these local EDPs are most likely to observe failure in the model first, their σ_{FEM} values are largest since the FEM models with the local column model have a defined failure during simulation. This means models without the local column model may have unrealistic demands in the simulation process leading to much larger EDP values. Comparing the global versus local, the local σ_{FEM} values are observed to be much larger than the global values, their averages being 0.88 and 0.44, respectively. This may be attributed to the change in local models within the four FEM used in this study. The t-test also relates to the σ_{FEM} values obtained. Most statistical similarities were observed in the first regression line from the data, coinciding with the lower range of IMs used to find the σ_{FEM} . The differences among the four modeling approaches are similar in the elastic range while major differences are observed while undergoing post elastic deformations under higher values of IM.

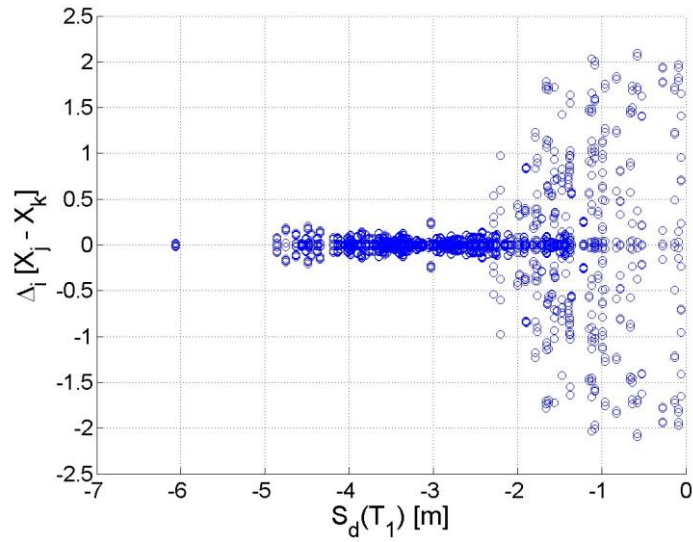


Figure 3.8 - Scatterplot of calculated variation data of shear EDP vs. natural log of spectral displacement.

Table 3.4 - σ_{FEM} data for each EDP at values less and greater that $\ln[S_d(T_1)] = -2.5$.

EDP	$\sigma_{FEM,1}$ @ $\ln[S_d(T_1)] \leq -2.5$	$\sigma_{FEM,2}$ @ $\ln[S_d(T_1)] \geq -2.5$
θ	0.06	0.56
St. Acc.	0.03	0.32
$\epsilon_{c \text{ col}}$	0.04	1.45
$\epsilon_{s \text{ col}}$	0.20	0.86
$\epsilon_{c \text{ beam}}$	0.05	0.41
$\epsilon_{s \text{ beam}}$	0.54	0.80
V_{col}	0.05	0.67
M_{col}	0.04	0.05
ϵ_{ext}	0.01	1.22
ϵ_{int}	0.01	1.24
Average	0.10	0.76

3.5. Component Fragility Curves

Typically probabilistic risk assessments for structural systems are assessed by developing fragility curves. Fragility curves are formulated from the variables that are derived in linear and bilinear PSDMs, as mentioned in section 3.4.1. These fragility curves calculate the probability that a demand exceeds a specified capacity given an IM used in the study. The fragility curve expression can be written as:

$$Fragility = P[Demand \geq Capacity | IM] = 1 - \Phi \left(\frac{\ln(C) - \ln(D(IM))}{\sqrt{\sigma_{D|IM}^2 + \sigma_M^2 + \sigma_C^2 + \sigma_{FEM}^2}} \right)$$

Equation 3.7 - Fragility expression.

Where Φ is the standard normal cumulative distribution function, $\sigma_{D|IM}$, σ_M , σ_C , and σ_{FEM} are lognormal standard deviation values that are defined as record-to-record uncertainty, modeling uncertainty, capacity uncertainty, and FEM uncertainty. The variables of C and $D(IM)$ are representative of the median of the capacity and demand, respectively. The capacity limit states may be seen in Table 3.5 These are used in accordance with equation 3.7 to develop fragility curves for local EDPs. The limit states considered are standard yielding and failure characteristics of steel and concrete, calculated shear and moment capacity of the column design, and a joint yielding strain discussed by Celik (2007).

Table 3.5 - Limite State Capacities for use in fragility analysis

Limit State	Symbol	Capacity
Concrete crushing strain	ϵ_c col; ϵ_c beam	0.004 (Berry 2003)
Steel yielding strain	ϵ_s col; ϵ_s beam	0.00138
Steel ultimate fracture strain	ϵ_s col; ϵ_s beam	0.10
Column shear	V_{col}	13.5 Kips
Column moment	M_{col}	850 Kip-inches
Joint yielding strain	ϵ_{ext} ; ϵ_{int}	0.005 (Celik 2007)

Fragility curves are estimated for ten different limit states, as seen in Appendix B, taking into consideration limit states on beams and columns. Although strain limit states for concrete and steel are presented for both columns and beams, the moment and shear limit states are only presented for the column since non-ductile RC buildings exemplify weak column-strong beam characteristics, as mention in Chapter 2. Figure 3.9 and Figure 3.10 are fragility curves for the moment capacity in a column on the first level of our three-story building. The difference between the two is the addition of the σ_{FEM} uncertainty parameter in the fragility calculations in Figure 3.10. Figure 3.9 is an example of the original fragility equation that does not include the newly proposed σ_{FEM} uncertainty developed in section 3.4.3. By adding the σ_{FEM} uncertainty, it may be seen that the resulting curves show the characteristic change in shape associated with a larger dispersion. As seen in Figures 3.9 and 3.10 and Appendix B, there is a significant difference between the usage of linear and bilinear PSDMs for fragility analyses. Bilinear is recommended for the local EDPs given the improvement in efficiency of the models. The use of bilinear PSDMs captures the non-linear demand characteristics of the EDPs. There is a trend in the bilinear curves of discontinuity at the intersection points of the

Y_1 and Y_2 regression lines. Bai et al (2011) also encountered this while running fragility analyses on bilinear PSDMs.

These fragility curves serve as tool for use in a risk assessment for the components in a non-ductile RC building. They portray the areas in a non-ductile RC that need to be strengthened (retrofitted) for safety to the public and adjacent buildings in case of damage or worse, collapse. The fragility curves of all the components may be viewed in Appendix B. By studying these fragility curves, it is observed that column moment and shear, Figure B.7 and Figure B.8, and the exterior and interior joint, Figure B.9 and Figure B.10, exhibit the highest probabilities of failure during an earthquake event. By taking into consideration the bi-linear behavior of the PSDMs, the column moment and column shear bi-linear fragility curves seem to plateau at a value less than 1.0 (complete probability of failure). This may be attributed to the modeling techniques used in this study for estimating the fragility curves. The joint strain capacity may be reached before the shear and moment capacity of the column, prohibiting the shear and moment capacity to achieve maximum response. It is also observed that column and beam steel tensile strain, Figure B.3 and Figure B.4, show a high probability of failure. The steel tensile strains observed in the columns may be early indicators that the columns are reaching their capacity in moment and shear. The fragility curves formulated in this study show that columns and joints in non-ductile RC buildings should be strengthened in order to reduce the probability of failure during an earthquake event.

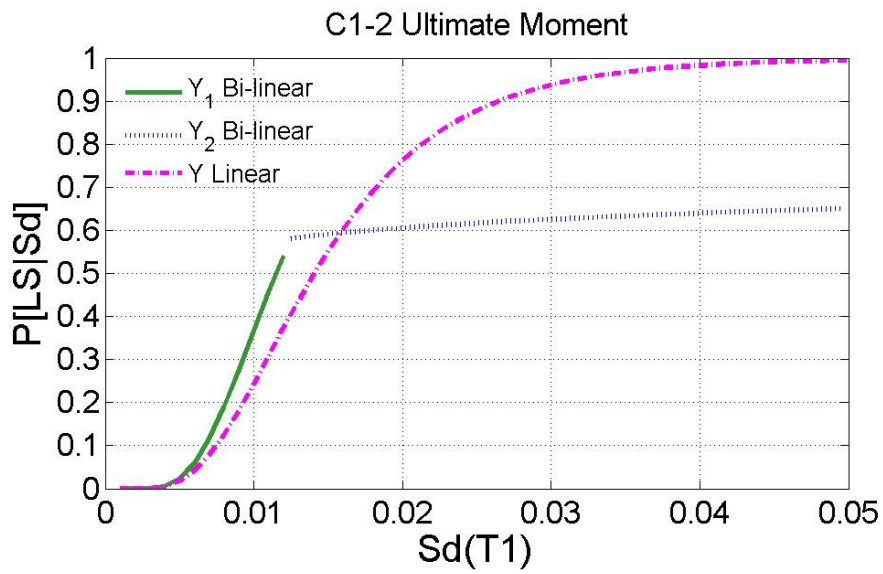


Figure 3.9 - Ultimate moment fragility curves for columns on first level; these fragility curves are calculated not including the σ_{FEM} uncertainty.

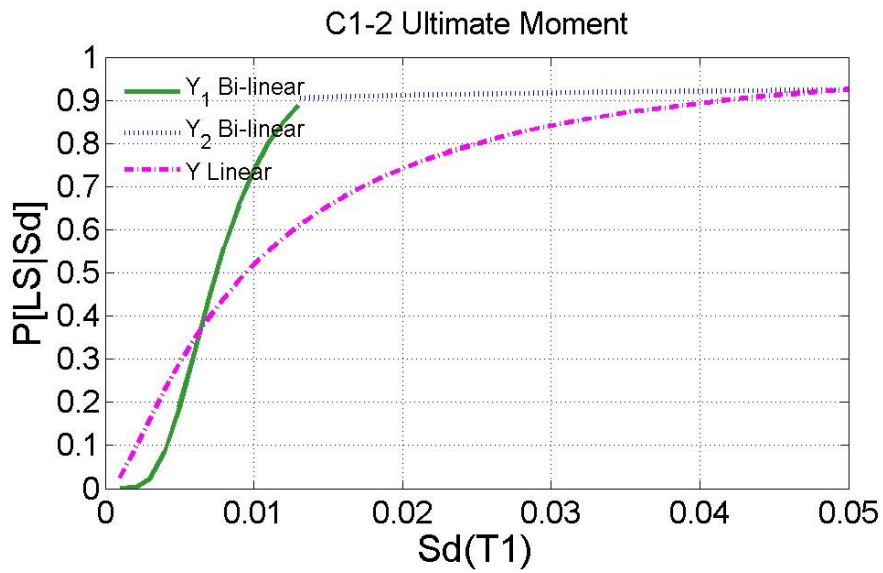


Figure 3.10 - Ultimate moment fragility curves for columns on first level; these fragility curves are calculated including the σ_{FEM} uncertainty.

Rapid Evaluation Survey of Earthquake Damaged Reinforced Concrete Components

4.1. Introduction

Fragility analysis offers one key ingredient of a risk assessment for non-ductile reinforced concrete buildings. However, for risk modeling to capture the impact of RC component damages, additional consequence modeling is required. One consequence of damage to non-ductile RC buildings is the potential loss of functionality due to post-event tagging of the structure, implying that it is unsafe for operation. As seen in section 2.4, tagging of buildings is becoming a normal procedure throughout the world. To better understand and model outcomes from the rapid evaluation process of tagging an individual building, a web-based survey has been developed. The survey is designed in order to capture rapid evaluation decisions of inspectors following an earthquake event who lack details on the structure being viewed. The survey presents individual components that exhibit seismic damage typically seen in reinforced concrete buildings.

Each damaged component is then followed by a series of question that pertain to the tagging decision, repair strategy, cost and duration of repair, suggested retrofits, and comments based on the damaged component observed.

Initially, this chapter describes the organization and layout of the survey. The responses to the web-based survey are then presented and discussed. The survey data is analyzed to provide probabilities of achieving various tagging decisions, and supplemental information on potential repair actions that affect closure time and costs. The demographics of the respondents are analyzed and presented to show the variation in profession, geography, and level of experience; and the correlation between the responses and demographic data is tested. Finally, a comparison is presented between the models derived from statistical analysis of the survey data and past earthquake tagging data of RC buildings from Loma Prieta. The chapter ends with concluding remarks and recommendations for future research that can build on this study or benefit from the resulting data collected.

The type of damages considered in the survey were identified within the typical damages mentioned in Chapter 2. Also, damages observed in the past Loma Prieta field reconnaissance and tagging files were considered for the survey. The consequence models that result from the study presented in this chapter can be integrated with component level fragility curves such as those presented in Chapter 3. The results of the survey will act as a tool to enhance the risk assessment of non-ductile RC buildings.

4.2. Web-based survey organization

The survey was put together using technical language common to engineers and inspectors whom may take part in a rapid evaluation of reinforced concrete buildings after an earthquake event. Prior to distribution, several engineers from academia and the industry were asked to review the survey for content and clarity, and it was adjusted in order to obtain more complete and detailed results. One major concern for the survey was the time needed to answer sufficiently. Since the survey was being distributed to busy professionals, it was modified to be finished within an average of thirty minutes after opening while still allowing for clear and comprehensive data collection. For those participants that do not have time to finish the survey, the web-based survey saves their inputs and allows them to finish at a later time or to submit a partially completed survey.

The survey is laid out in multiple pages. Each page represents a new area of concern for the respondent, such as consent for participation in the survey, personal information to be kept confidential and used for survey demographic reasons, and answering rapid evaluation questions pertaining to component type damages typical in reinforced concrete buildings. By splitting the survey into separate pages, it allows the web-based survey to save answers as the respondent proceeds to the next question and gives the respondent a sense of progress to completion of the survey. A screenshot from the web-based survey is shown in Figure 4.1. Figure 4.1 is an example of a typical question regarding rapid evaluation of component damage in a reinforced concrete building, particularly at the joint in this example. Each section of the survey follows this layout, with the images (Figure 4.1a) (NISEE) being shown ahead of a set of questions

(Figure 4.1b) to be answered in response to the general damage observed in the set of images. Care was taken to prepare each section of the survey so the respondent would not have to scroll up or down while answering a set of questions relating to the damaged component. This presentation type in surveys, where all questions pertaining to a set of figures are located in the survey taker's view, was studied by Dillman et al. (1998a) and Baatard (2012), and found to be most effective for gathering web responses from the survey participant.

Five major types of damage were presented in the survey for judgment: column shear, spalling, joint damage, column flexure, and beam damage, each with two subtypes. The first subtype represented minimal damage, i.e. cracking, while the second subtype represented a more obvious sign of structural damage, i.e. rebar buckling around cracked concrete. These were selected based on their commonness of occurrence as well as their visibility. Such elements would easily be seen by inspectors and thus would have significant influence on the tagging outcome. For each damage subtype, survey-takers were shown pictures of affected components and asked to suggest which tag the building might receive based off of the images. The four tags, which follow the ATC-20's (1989) recommendations, were green, which signifies a safe structure, yellow, which signifies that only limited entry should be allowed, red (repairable), which signifies the structure should not be entered but it could be recovered, or red (demolition suggested), which is similar to the previous tag except the building probably would not be recoverable (1989). Following this, the survey included open-response sections, which asked for element repair strategies and estimates of their costs/durations. Participants were also given space to comment on their

responses. The addition of an open-ended comment to each section was valuable to be able to understand the perspective of the participants.



(a)

Please provide answers most representative of the group identified in Figure 1, and if any case does not fit within the group you may identify it in the comment box:

1a. Suggested "tag" in post-earthquake evaluation:
 Green Yellow Red (repairable) Red (demolition suggested)

1b. Recommended repair strategy to restore damaged component to its original state:
Remove loose concrete, repair rebar, recast with concrete

1c. Referring to your response in question (1b), approximate:
Duration of repair, including design (months): 1
Costs of repair (\$): 50000

Comments referring to responses given in questions (1b) and (1c):
The second photo indicates a more critical situation relative to photo 1. If several columns looked like photo 2, the building would likely be given a red tag. The cost of repair would be for multiple column repair.

1d. What preventive retrofit measure(s) could have been taken, prior to the earthquake, to mitigate this type of damage?
More confinement steel in the joint.

(b)

Figure 4.1- Screenshots of a typical section from the online survey, which includes: (a) images demonstrating one of five different types of component damage due to earthquakes (joint damage in this case) and (b) questions pertaining to the images. Examples of responses are depicted for the post-earthquake evaluation tagging and open-ended questions concerning repair possibilities, estimated time and cost of these repairs, preventative measures, and additional comments.

4.3. Results

4.3.1. Demographic Analysis

This survey was intended principally for professionals with knowledge of reinforced concrete building characteristics and experience in post-earthquake event inspections. To reach this target audience, the survey was distributed through various networks such that it might reach practitioners with relevant experience. For example, it was distributed via the ASCE/SEI Seismic Effects Technical Activities Committee, the Earthquake Engineering Research Institute list serve, among other contacts who were asked to distribute it to their network. The overall response rate is unknown due to the challenge of identifying how many people actually received the survey link, and the fact that each recipient in a mass distribution list was not in the target audience of qualified professionals. However, there was a response rate of 40% for those participants who entered into the survey and completed the survey. There were 98 total participants, of which 39 left significant responses after the initial “personal information” page. Thirty-seven of these were determined to be qualified based on the background information they provided, mainly experience with earthquake/structural engineering; the results of this survey are based on their responses.

Regarding the occupations of survey participants, two key groups could be formed. The first is comprised of professionals with industry affiliations, representing 62% of the respondents while participants with affiliations in academia made up the remainder. Those working in industry had positions such as principals and project engineers. While 64% of the participants in academia were professors (assistant, associate and full), the rest were researchers and lecturers. Approximately 60% of the

respondents were US based, while others were located in different countries, such as India, Mexico, and elsewhere.

When asked to rate their level of experience on a scale from 1 to 10, with 10 signifying 100+ hours of experience, those in industry described themselves as having higher levels despite years of professional experience being similar, as seen in Table 4.1. As indicated in Table 4.1, the overall pool of respondents had average of 23.3 years of professional experience with a rating level of relevant experience that averaged 7.6 with a median value of 10. These statistics indicate a reported competency concerning the subject. Furthermore, while not reported in the table, the modal value of experience with post-earthquake inspection from the pool of respondents was 10, suggesting a high level of not only training but field experience with post-earthquake evaluation or tagging of buildings. The potential correlation of such demographic features and survey responses are further tested in the subsequent chapter sections.

Table 4.1 - Experience of survey participants from different occupational backgrounds.

	Number of Respondents	Post-Earthquake Level of Experience (1-10)		Years of Professional Experience	
		Average	Median	Average	Median
Industry	23	8.6	10	23.7	28
Academia	14	5.9	5.5	21.3	23
Total	37	7.6	10	23.3	25

4.3.2. Post-Earthquake Evaluation Tagging and Repairs

The resulting survey data was analyzed to quantify the probability of a particular tag being assigned to the building given the presented visual or observable level of

component damage. It is acknowledged that in the field the inspector will have access to observe combinations of component damage when assigning a tag. Hence the responses offer a potential tag assigned even in the absence of other observable component damage. The last page of the survey posed a question to gain insight into any difference in system level tag assigned due to combinations of component damages, as further discussed below. In addition to deriving “conditional tagging probabilities,” or likelihood of tag assignment given component damage, an average tagging score is presented below. To facilitate this reporting, each tag color was assigned an equivalent score: 1 for *green*, 2 for *yellow*, 3 for *red (repairable)*, and 4 for *red (demolition suggested)*. A numerical average could then be calculated. This section provides the results of the statistical analysis of tagging responses, tests of the correlation between survey responses and demographic data of the respondent, and on insights from the corresponding repair model responses for each type and level of damage.

The first damage type presented in the survey was related to shear performance of reinforced concrete columns. Figure 4.2 presents an example of one level of damage presented in the survey (i.e. observable X-cracking in the columns) and the conditional tagging probabilities derived based on survey responses on column shear behavior for both minor cracking and X-cracking suggesting a shear failure. For minor cracking observed in reinforced concrete columns, there was some inconsistency in the tagging; but overall the results suggest that the building would be safe for at least limited entry with 73% of the tagging responses either *green* (30%) or *yellow* (43%).

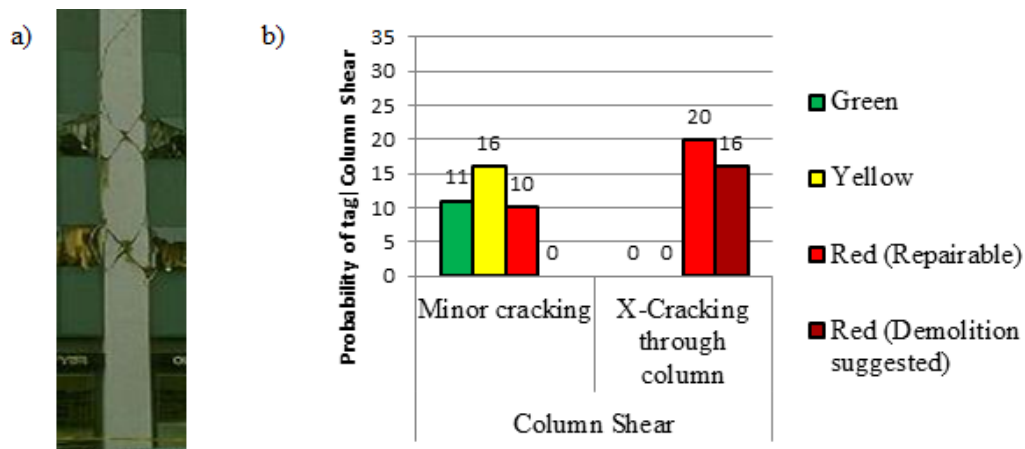


Figure 4.2 - (a) An example of X-Cracking through a multi-story building column shown in the survey. (b) Probabilities of two column shear damage types receiving tags.

Table 4.2 presents the number of responses given by the respondents for each type of damage observed in the survey. The most common repair strategy of epoxy injection, as seen in Table 4.2, implies minimal damage and the potential for a rapid repair. For the second group of images, X-cracking was observed through different columns as shown in Figure 4.2a. With an average tag of 3.4, most respondents agreed there is significant damage that would render the buildings inaccessible and possibly irreparable (44% of tags). The respondents whom tagged *red (repairable)* suggested a complete replacement by recasting the columns and replacing the damaged reinforcement.

The next damage type presented in the survey dealt with spalling of columns in a RC building. Tagging for spalling was the most uncertain of all the damage types, as is displayed in Figure 4.3b. Spalling on the columns and joints were both considered in the survey. The most common repair strategy for spalling at the columns and joints is recasting the concrete. Based upon the additional comments provided by the respondents in the comment field, the respondents found spalling on columns, as well

as joints, to be minor, superficial damage but possibly indicative of larger problems. This would explain the *yellow* (50%) and *red (repairable)* (35%) tags.

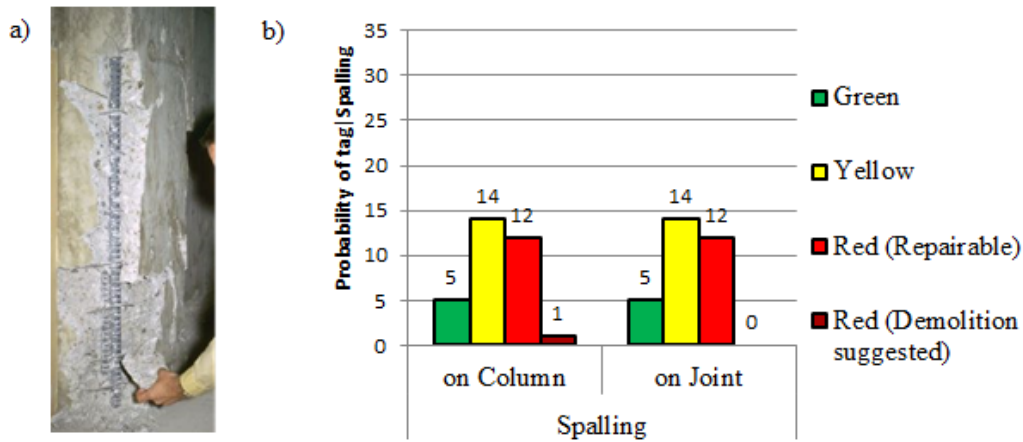


Figure 4.3 - (a) An example of spalling on a column shown in the survey. (b) Probabilities of column and joint spalling receiving tags.

The performance of joints in RC buildings is of great importance to post-earthquake inspections. Joints represent the regions where loads are transferred to other regions in the structure. Joint damage beyond spalling was tagged quite consistently, resulting in the lowest level of uncertainty in tagging decision based on the observed damage. Both cracking on the joint and observation of rebar backing were considered. When rebar is visible and buckling within a joint, as shown in Figure 4.4, there is a 97% probability of both *red (repairable)* and *red (demolition suggested)* tags. For numerous large cracks in a joint, *red (repairable)* and *red (demolition suggested)* made up 81% of tags. Among the few participants who tagged joint cracks with *yellow*, several noted in their comments that they were only referring to one of the two pictures shown with smaller cracks and specified that the other picture deserved a *red* tag in their comments. As seen in Table 4.2, some repair strategies were suggested, mainly recasting and adding reinforcement.

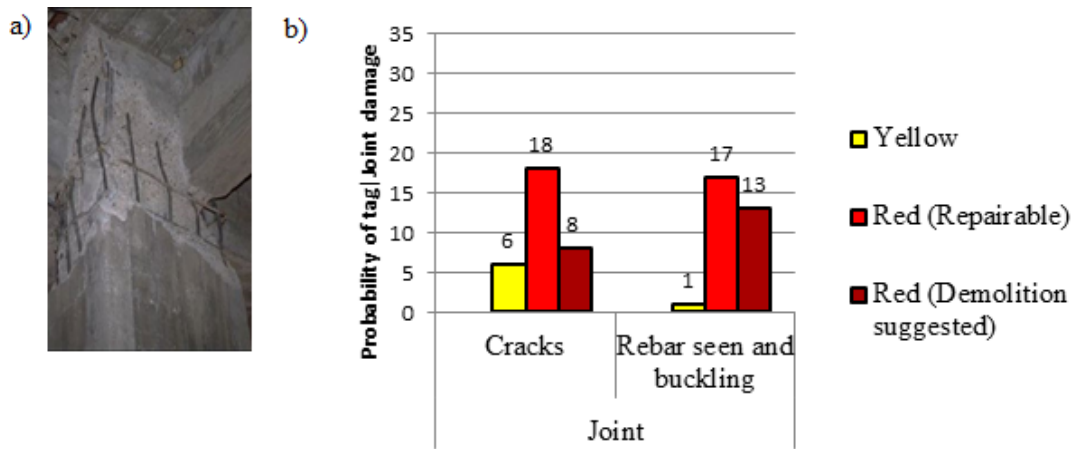


Figure 4.4 - (a) An example of rebar seen and buckling on a joint shown in the survey.
 (b) Probabilities of two joint damage types receiving tags.

Column flexural damage was considered in two different manners: in terms of plastic hinging, with concrete crushing and rebar buckling, as well as residual drift. Both cases received only *red* tags, indicating that they signify possible structural failure or unsafe entry and should be considered hazardous. There was some difference in opinion as to whether the column shown in Figure 4.5a would be capable of restoration; 55% of respondents believed it could be replaced after shoring, but the rest seemed to believe demolition would be preferable, especially if more columns were in a similar condition. In situations where the columns were no longer plumb, 94% of participants recommended complete demolition while the rest stated that reparation would be possible only at great difficulty and expense.

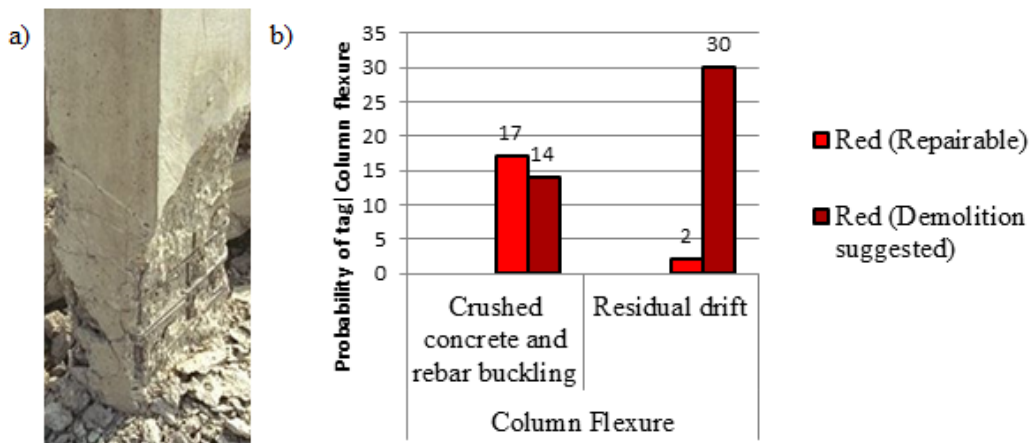


Figure 4.5 - (a) An example of crushed concrete with rebar buckling at the base of a column shown in the survey. (b) Probabilities of two types of column flexure damage receiving tags.

The last set of component damages focused on the performance of beams, depicting minor cracking or flexural hinging of beams. The picture was somewhat out-of-focus and may have caused some confusion, but generally the results were rather clear. 52% of participants tagged minor cracks in a beam with *green*, 38% with *yellow*, and only 10% gave this damage type a *red* tag. Respondents largely considered this to be trivial damage capable of being repaired quickly and simply with epoxy injection. Flexural hinging, shown in Figure 4.6a, was considered much more serious; 18% gave *yellow* tags and 57% gave *red (repairable)* tags, and the rest recommended demolition. The most common repair strategy was complete replacement (41%).

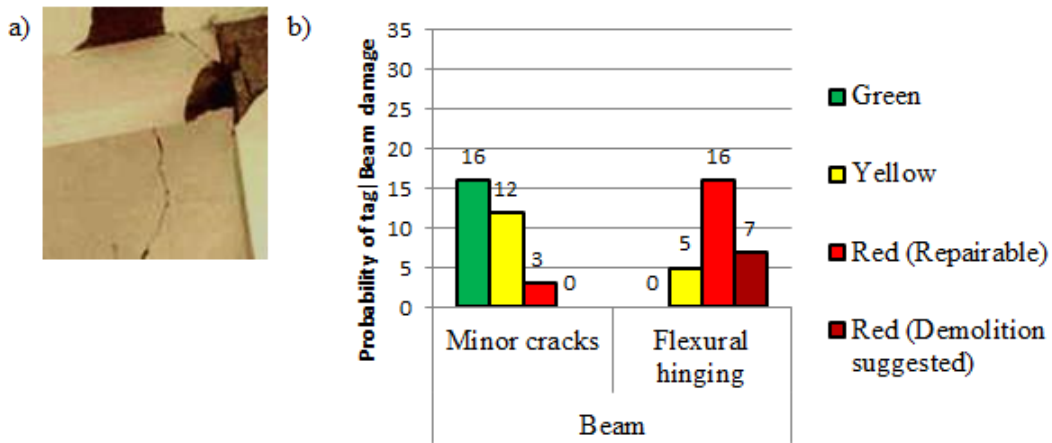


Figure 4.6 - (a) An example of flexural hinging in a beam shown in the survey. (b) Probability of two types of beam damage receiving tags.

The correlation between demographic data and response tendency was investigated for different features. Such correlations could be valuable in understanding how different inspectors might evaluate a building based on their backgrounds. The following demographic features were examined: post-earthquake experience level, academic vs. industry affiliation, being located in the U.S. vs. outside of the U.S., and years of professional experience. Both correlation coefficients and differences in mean tagging scores between populations were tested. In general the analysis suggests a relatively weak correlation between most features and responses (e.g. correlation coefficient on the order of 0.3), but interesting trends did appear. For instance, a relationship between the level of experience and the tagging approach was seen: participants who labeled themselves as having 100+ hours of experience were more likely to tag elements in a safer tagging category as compared to other participants. Except for one damage type in which all participants tagged nearly the same, the score for those with 100+ experience hours was on average 10% less than those with lower levels of experience. Similarly, participants from the U.S. or in industry were not as conservative as their counterparts and tended to give tags with lower ratings. The

average tag score for those in industry was about 10% lower than those in academia, and the average for those in the U.S. was 13% lower than those outside of the U.S. Furthermore, some of the larger magnitudes of correlation (e.g. on the order of 0.6) indicated that spalling, a controversial damage type, was judged more harshly by those from the international community and from industry.

Although the primary emphasis of the survey was on rapid inspection, some estimates were provided for the potential duration and costs of repairing the damage types to single elements, shown in Table 4.3. The mean, median and mode were calculated for each factor, noting that wide variation in responses are observed as expected since the respondents were not provided with details on the building or component design nor sufficient time for refined cost estimation. Median values are used as a statistic for discussing the resulting estimates from the respondents, and rather than absolute values the responses are recommended to be considered in relative terms. The figures with the least variation were for minor cracks in columns and beams as well as spalling, which would all similarly take about 1-2 months and cost not much more than \$2500-5000. Responses for other damage types were fewer and thus less certain. In general, most trends in increasing level of damage to a component resulted in larger median values of cost and duration, as expected, with the exception of the joints which suggests some lack of reliability of the data for these components. The median duration of repairs were suggested to linearly increase for column minor cracking, spalling, and X-cracking from shear failure. The flexural hinging of beams was suggested to take about twice as long to repair at four times the cost of minor cracking. Residual drift, or out of plumb columns, was deemed highly unlikely to repair. It is suggested that refined cost and duration estimates for building specific studies can be

derived considering the prospective repair strategies identified above from the survey, and result in superior cost and time estimates with less uncertainty.

4.3.3. Comments

The survey was set up to allow comments about the separate sections and answers to open ended questions. The comments are important to acknowledge, as they raise valid concerns related to the survey material or responses. For example, some respondents were hesitant to provide cost and duration estimates since they acknowledged that the survey does not provide specific details on the building, size of the earthquake (which may affect labor and materials availability), and number of damaged components. Most did not let this prevent them from tagging the pictures, however, which was the primary survey aim given its emphasis on rapid post-event evaluation.

The results showed some variation for the tagging of various component types and damage levels. However, it must be stated that the uncertainty in tagging probabilities cannot be fully attributed to variation in inspector opinion. Some lack of uniformity may also be attributed to a lack of clarity in the photos, variation in potential decisions for different example images provided for the same damage type, or a possible misunderstanding of the tagging procedure. One example is the aforementioned variation in responses that multiple respondents noted regarding images provided for joint cracking that may result in different recommendations.

Another comment box further helped obtain opinions on which precautions could be taken to reduce these types of damage. An open-ended question asked “What preventive retrofit measure(s) could have been taken, prior to the earthquake, to

mitigate this type of damage?" Many respondents agreed that some of the damages were expected and designed to act as they were presented in the survey. These damages included the spalling on the column and joint and minor cracks on the column. They mentioned that not much should be done in terms of retrofit, but ways of strengthening these components are FRP wrapping and jacketing. Some respondents mentioned that better initial designs of the building before construction would have mitigated many of the damages seen in the survey. The three retrofit measures mentioned by most were FRP wrapping, jacketing, and shear wall installation to strengthen and stiffen the individual components and the overall building.

From the feedback, some participants also noted the challenge of tagging based upon observation of individual components, without knowledge of the condition of the entire building. In its current format the main pages of the survey are intended to understand if an inspector would tag the building a particular color upon observing a given component damage level shown throughout the survey. The final page of the survey was set up to address this challenge, as a practical compromise to showing the many permutations of possible combinations of component damages observed in a building. Respondent were asked to select (with checkboxes) which combinations of component damages would lead to a *red* tag of the building, eliminating the case of any single components that lead to a *red* tag. This question amassed very little response. It cannot be definitively inferred if this indicates that no additional combinations of component damages typically result in a red tag, other than those that already include a single component that would warrant the same closure decision; or if the question was unclear. For the participants that did respond, the only combination that would

potentially warrant a *red* tag was spalling in a column or beam along with minor X-cracking in the beam.

4.4. Comparison with Empirical Data

The results of this survey were compared to empirical evidence gathered from the 1989 Loma Prieta earthquake in order to provide a basic assessment of the tagging tendencies suggested by the survey relative to the actual tags assigned following a real event and noted component damage levels. Inspection files were collected and analyzed from the San Francisco Department of Building Inspection. These files included the ATC 20 Rapid Evaluation Forms and supplementary material such as follow up inspection, recommendations, and tagging changes. Of the files accessed, 18 reinforced concrete buildings were found to be either *yellow* or *red* tagged after the Loma Prieta earthquake in the San Francisco area with paper based inspection files maintained. Table 4.4 gives a short summary of the data collected from the Loma Prieta files: the initial tags given to RC buildings, the first tag change made after further more detailed inspection, the duration of time between the initial tag and the first tag change after initial tag, the number of structures in each tagging category, and the percentage of buildings in each initial tag category that sustained particular damages. Most damages observed in the Loma Prieta earthquake are present in the survey, such as spalling, minor cracks, and story lean. The tags given to buildings after the Loma Prieta earthquake are similar to the survey results. It is noted that the survey does not cover all forms of damage that were reported and may be observed for RC buildings—a compromise made upon rounds of survey feedback and revision to enable efficient completion.

Table 4.2 - Suggested repairs from survey.¹

		Epoxy Injection	Recast	Add Reinforcement	Recast + Replace Reinforcement*
Column Shear	Minor cracking	22	5	0	1
	X-cracking through column	0	3	0	12
Spalling	on Column	5	20	1	1
	on Joint	2	16	1	0
Joint	Cracks	2	6	2	6
	Rebar seen and buckling	0	3	1	9
Column Flexure	Crushed concrete and rebar buckling	1	1	2	11
	Residual drift	-	-	-	-
Beam	Minor cracks	12	0	1	0
	Flexural hinging	1	4	2	11

¹ this repair strategy signifies replacing the component.

Table 4.3 - Number of responses, duration (months), and costs (\$) of repairs with mean, median, and mode values.

		Duration (months)			Cost (\$)			Number of Responses	
		Mean	Mode	Median	Mean	Mode	Median	Duration	Cost
Column Shear	Minor cracking	2	1	1	6960	1000;5000	2750	23	18
	X-cracking through column	3	3	3	4250	5000	5000	4	4
Spalling	on Column	2.1	1;2	2	8670	1000;5000	4000	19	14
	on Joint	2.8	1	2	11560	3000	5000	19	15
Joint	Cracks	3.1	1;2;6	2	17000	1000;3000; 10000;50000	10000	10	9
	Rebar seen and buckling	2.7	1;2	2	15000	2000	6000	7	6
Column Flexure	Crushed concrete and rebar buckling	3.4	1	2.5	17670	2000;5000; 50000	10000	9	9
	Residual drift	-	-	-	-	-	-	0	0
Beam	Minor cracks	1.9	1	1	4110	1000	2250	14	12
	Flexural hinging	2.4	1	2	14890	25000	8000	9	9

The observed damage identified as “Column” in Table 4.4 refers to damage beyond the severity of spalling such as flexure-shear behavior. As seen in the survey results, structures with this kind of column damage were all given *red* tags initially. Structures experiencing story lean, or residual drift, were also consistently tagged *red*, comparable to the survey. Sixty-six percent of the demolished RC buildings experienced story lean and 50% of buildings with story lean were ultimately demolished. Minor cracks and spalling damages showed the most variation, as both were present in buildings being tagged with a *red* or *yellow* tag initially. These results are similar to those from the survey in which participants displayed high uncertainty. After further inspection of the *red* tagged buildings from Loma Prieta, some RC buildings were changed to *yellow* while others were ultimately demolished. This type of change in tag corresponds to the *red (repairable)* and *red (demolish)* tag choices given in the survey. Observed damages defined as “Falling Debris” and “Wall Crack” were added to Table 4.4 to present the overall identified damages. Falling debris presented a major safety threat to occupants of the RC buildings being inspected.

Past tagging records provide the study valuable real world data to compare directly with the survey responses. From the data observed in Table 4.4 and the comparisons noted above, it is evident that the data obtained from the survey is similar in many ways to the Loma Prieta files. For instance, RC buildings with observed “Column” damage were consistently tagged *red* in the Loma Prieta files, while the survey respondents indicated that observed “Column” damage, whether in the form of flexure or shear, would also warrant a *red* tag. Also, both the survey and

the Loma Prieta files display larger uncertainties in tagging decisions for damages such as spalling and minor cracks. While it was a challenge to locate tagging files from past earthquakes, this survey is meant to compliment any future data that may be collected from future earthquake events. The survey provides an opportunity to be compared with future tagging data gathered from earthquake events.

Table 4.4 - Tagging and damage data of RC structures after the Loma Prieta earthquake.²

Initial Tag	1 st Tag Change	Count	Duration* (months)	Percent of Observed Damage Noted by Inspector					
				Falling Debris	Minor Cracks	Wall Crack	Column	Spalling	Story Lean
Red	Yellow	9	1.2	78%	66%	22%	56%	56%	22%
Red	Demolished	3	16.5	66%	66%	0	100%	66%	66%
Yellow	n/a	6	-	83%	66%	50%	0	66%	0

² Duration from Initial Tag to 1st Tag Change

Conclusions and Future Research Opportunities

5.1. Summary and Conclusions

Numerical modeling processes, as seen in Chapter 3, are becoming increasingly relevant in research and industry to gather response data for chosen design and load patterns applied, and to support structural vulnerability modeling subjected to extreme events like earthquakes. In this thesis, a non-ductile RC building was modeled based on the design of an experimental setup to compare and validate the results. In the study, joint and shear component models were applied to the numerical model to observe whether these added components may provide a better approximation to the experimental results. From the analysis conducted, comparisons were made between the resulting probabilistic seismic demand

models and a new epistemic uncertainty σ_{FEM} was quantified to represent the uncertainty observed by using various finite element modeling approaches.

Four combinations were adopted, referred to as *rigid*, *joint*, *column*, and *joint-column models*. After performing lateral load analysis to interior and exterior subassemblages and applying scaled Taft Earthquake ground motions to the full scale numerical models, the models with the incorporated *joint model* proved to be the most accurate as compared to the experimental results. For the subassemblages, there was a 5% improvement in predictive abilities for the *joint models* as compared to the *rigid model*. Also, the *joint models* have more accurate representations of pinching and strength degradation in the force-deformation response of the subassemblages. The peak deformation responses of the time history displayed differences of 31% for *rigid model* as compared to 20% for the *joint-column model*. Hence, the addition of the component models in the subassemblage and full scale models provide more related approximations for comparison to the experimental data. The components models are also able to record local engineering demand parameters. The new finite element modeling uncertainty value (σ_{FEM}) was quantified from a probabilistic seismic demand analysis. The σ_{FEM} arises from the variation of demands observed between the four different numerical models used for the probabilistic assessment. The σ_{FEM} is found to be on average 0.11 for the lower range of ground motion intensity measures (IMs) and 0.69 for the upper range of IMs. The σ_{FEM} helps establish a relationship between the various FEM techniques used in research and industry.

Fragility curves were developed using the linear and bilinear PSDM data gathered from the analyses. The use of bilinear PSDM data provides a more efficient way of capturing the non-linear behavior of the local EDPs. The fragility curves were evaluated for local EDPs such as column concrete strain, column shear, and interior joint strain. A direct comparison was made by adding the σ_{FEM} uncertainty into the fragility curve equation (3.7), as seen in Chapter 3.5. Figures 3.9 and 3.10, as well as figures in Appendix B, plot the direct comparison of linear vs bilinear fragility models. Figures 3.9 and 3.10 provide a comparison with the addition of the σ_{FEM} uncertainty. The curves with the added σ_{FEM} uncertainty display the characteristic expected of a fragility model with larger dispersion. Looking in Appendix B, the largest vulnerability of a non-ductile RC building lies in the columns and joints, as seen in Figures B.7, B.8, B.9, and B.10. Straining of the steel rebar also has a large probability of failure, as seen in Figures B.3 and B.4. As expected in a non-ductile RC building, the column and joints are most susceptible to damage during an earthquake event.

Fragility modeling using finite element models provides one tool that may be used in a risk assessment. To enhance the risk assessment, there needs to be an understanding of the consequences that arise from the damage of non-ductile RC building components. These consequences may arise in the form of potential for loss of life, duration of closure due to a component needing to be repaired or replaced, and the costs related to the damage. Chapter 4 focused on the rapid evaluation of reinforced concrete buildings after an earthquake event. By presenting common damages observed in reinforced concrete buildings in a web-based survey

format, the study is able to capture tagging decisions, and supplemental recommendations to support repair modeling from experts in the field. It is critical to understand that many qualified inspectors deployed after earthquake events have different backgrounds and see damages in structures differently from one another, which may result in variation in tagging outcomes. Through analysis of the collected survey data, this study supports uncertainty modeling for seismic risk assessment of reinforced concrete buildings, recognizing that potential tagging outcomes constitute an important but uncertain decision variable for motivating such factors as investment in retrofit, heightened level of seismic design, or estimation of indirect losses which may be affected by building closure. Of the 37 survey responses considered in the analysis, participants were spread along various demographic areas: industry vs. academia; located in the US vs. located outside the US; 100+ hours of post-earthquake experience vs. <100 hours; located in seismic region vs. not located in seismic regions. Overall, however, the pool of respondents can be characterized as a group with a median of 25 years of professional experience with a self-proscribed post-earthquake inspection experience level of 10, on a scale of 1-10. The feedback from such a group can provide key insights into tagging probabilities and associated repair models.

A main outcome of the survey and response analysis was quantification of the likelihood that a reinforced concrete building will be tagged a particular color (*green, yellow, red (repairable), red (demolition suggested)*) based upon the inspector's observation of a component showing damage. Component damages that showed buckling of the steel reinforcement and/or cracks that extend completely

through the beam, column, or joint typically warranted a *red* tag. The damaged components that only showed minor signs of cracking or spalling tended to garner the largest uncertainty in tagging decisions, with most of the tags being *green* or *yellow* but with a small percentage tagged *red* until further inspection of the entire building and review of details of the component section. The survey results can be used to identify which component damages alone tend to warrant a particular tagging decision upon rapid field investigation, and support probabilistic performance assessment of RC buildings based on anticipated closure decision. As described in ATC-20 (1989), the tagging assignments in the field are typically based on observations of component damage and on the perceived overall condition of the structure, suggesting that individual component damages provide only a first step to improved closure and repair modeling. While the survey was designed to address this issue as well, little response was amassed from the inquiry regarding any additional combinations of component damage that may warrant a different level of building tag beyond that of the worst component identified in the survey. Some participants did indicate that the combination of column spalling and beam cracking may warrant a *red* tag, while the observation of these component damages on their own may only garner a *yellow* tag. Beyond the tagging probabilities, the survey data also provides a collection of recommended repair procedures per component damages. These repair actions can form the basis of refined loss estimation, as work in this area is trending toward considering component level damage and repair cost models.

5.2. Future Research Recommendations

There is a lot of information presented in this thesis that may be developed even further in future research. The use of 2D finite element modeling was used in this study, but a 3D model may provide more insight into the realistic behavior of a non-ductile RC building. There needs to be more work done in determining how to implement the σ_{FEM} uncertainty into fragility modeling, since there are two regions of σ_{FEM} uncertainty in the bilinear PSDMs. It may be best to look into a polynomial function to quantify the σ_{FEM} uncertainty. While this study only looked at four various modeling techniques in the Opensees framework, the σ_{FEM} uncertainty may be updated with the addition of more models from various platforms. The σ_{FEM} uncertainty should be inclusive of all types of models that researchers and professionals use to conduct fragility analyses. While this study did not focus on retrofitting measures, retrofits should be studied in order to decrease the vulnerability observed in this thesis.

For future studies, the fragility curves estimated from the finite element analyses should be related to the responses of the survey, and there should be direct correlations between the fragility analyses and tagging. Beyond the analysis presented in this thesis, the fragility curves and survey data summarized can provide a basis for future seismic risk assessment and loss estimation of reinforced concrete buildings, where the relationship between component damage and anticipated closure and repair decisions are critical. While the survey presented in the thesis provides a first attempt to collect such response data in a scientific survey and

addresses a key gap in existing literature and risk modeling packages, a larger response pool is always desirable. Since the results suggested potential correlation between demographic data and tagging tendency future opportunities may exist to define refined tagging probability models based upon the anticipated makeup of the inspector group if it can be inferred for a structure or region. Future studies are also recommended to further explore the influence of component combinations on tagging assignment. Finally, the comparison with Loma Prieta post-earthquake inspection files provided a valuable opportunity to benchmark the survey responses with empirical data. As post-event data collection and preservation becomes more streamlined, additional opportunities may exist to perform not only comparative assessments between the survey and empirical data but also update the probabilistic models with field data.

References

- ACI-ASCE. (1976). Recommendations for Design of Beam-Column Joints in Monolithic Reinforced Concrete Structures. *Journal of The American Concrete Institute*, 73(7), 375-393.
- Alath, S., & Kunnath, S. K. (1995). *Modeling inelastic shear deformation in RC beam-column joints*. Paper presented at the Proceedings of the 10th Conference on Engineering Mechanics. Part 1 (of 2), May 21, 1995 - May 24, 1995, Boulder, CO, USA.
- Altoontash, A. (2004). *Simulation and Damage Models for Performance Assessment of Reinforced Concrete Beam-Column Joints*. (Doctor of Philosophy), Stanford University, Stanford, CA.
- Anagnostopoulos, S., Moretti, M., Panoutsopoulou, M., Panagiotopoulou, D., & Thoma, T. (2004). Post-earthquake damage and usability assessment of buildings: further development and applications. In a. C. P. E. European Commission-D.G. Environment (Ed.). Patras, Greece.
- Aslani, H., & Miranda, E. (2005). Probability-based seismic response analysis. *Engineering Structures*, 27(8), 1151-1163. doi: 10.1016/j.engstruct.2005.02.015
- ATC. (1989). Procedures for Postearthquake Safety Evaluation of Buildings *ATC-20*. Redwood City, CA: Applied Technology Council (ATC).
- Aviram, A., Mackie, K. R., & Stojadinovic, B. (2008). *Epistemic Uncertainty of Seismic Response Estimates for Reinforced Concrete Bridges*. Paper presented at the The 14th World Conference on Earthquake Engineering, Beijing, China.
- Aycardi, L. E., Mander, J. B., & Reinhorn, A. M. (1994). Seismic resistance of reinforced concrete frame structures designed only for gravity loads: Experimental performance of subassemblages. *ACI Materials Journal*, 91(5), 552-563.
- Baatard, G. (2012). A Technical Guide to Effective and Accessible web Surveys. *Electronic Journal of Business Research Methods*, 10(2), 101-109.
- Bai, J.-W., Gardoni, P., & Hueste, M. B. D. (2011). Story-specific demand models and seismic fragility estimates for multi-story buildings. *Structural Safety*, 33(1), 96-107. doi: 10.1016/j.strusafe.2010.09.002
- Baker, J. W., Lin, T., Shahi, S. K., & Jayaram, N. (2011). New Ground Motion Selection Procedures and Selected Motions for the PEER Transportation Research Program (pp. 106p).
- Bal, İ. E., Crowley, H., Pinho, R., & Gülay, F. G. (2008). Detailed assessment of structural characteristics of Turkish RC building stock for loss assessment models. *Soil Dynamics and Earthquake Engineering*, 28(10-11), 914-932. doi: <http://dx.doi.org/10.1016/j.soildyn.2007.10.005>
- Bracci, J. M., Reinhorn, A. M., & Mander, J. B. (1992a). Seismic Resistance of Reinforced Concrete Frame Structures Designed Only for Gravity Loads: Part I - Design and Properties of a One-Third Scale Model Structure. Buffalo, NY.

- Bracci, J. M., Reinhorn, A. M., & Mander, J. B. (1992b). Seismic Resistance of Reinforced Concrete Frame Structures Designed Only for Gravity Loads: Part III - Experimental Performance and Analytical Study of a Structural Model. Buffalo, NY.
- Celik, O. C. (2007). *Probabilistic Assessment of Non-Ductile Reinforced Concrete Frames Susceptible to Mid-America Ground Motions*. (Doctor of Philosophy), Georgia Institute of Technology, Atlanta, GA.
- Comartin, C., Bonowitz, D., Greene, M., McCormick, D., May, P., & Seymour, E. (2011). The Concrete Coalition and the California Inventory Project: An Estimate of the Number of Pre-1980 Concrete Buildings in the State: The Earthquake Engineering Research Institute; The Pacific Earthquake Engineering Research Center; The Applied Technology Council.
- Computers & Structures, I. (2013a). ETABS 2013 Overview. from <http://www.csiamerica.com/etabs2013>
- Computers & Structures, I. (2013b). SAP2000 Overview.
- Cornell, C. A., Jalayer, F., Hamburger, R. O., & Foutch, D. A. (2002). Probabilistic basis for 2000 SAC federal emergency management agency steel moment frame guidelines. *Journal of Structural Engineering*, 128(Compendex), 526-533.
- CPAMI, NAA, CUPCEA, CUPSEA, & PGEA. (2005). Post-earthquake damage evaluation guideline (M. o. I. Construction and Planning Agency, R. The National Association of Architect, C. U. o. P. C. E. Association, C. U. o. P. S. E. Association & P. G. E. Association, Trans.): Construction and Planning Agency, Ministry of Interior, The National Association of Architect, ROC, Chinese Union of Professional Civil Engineers Association, Chinese Union of Professional Structural Engineers Association, Professional Geotechnical Engineers Association.
- Dillman, D. A., Torta, R. D., & Bowker, D. (1998a). Principles for Constructing Web Surveys. Pullman, WA: Social and Economic Sciences Research Center (SESRC).
- El-Attar, A. G. W., R. N.; Gergely, P. (1991). Shaking Table Test of a One-Eighth Scale Three-Story Lightly Reinforced Concrete Building (Vol. Technical Report NCEER-91-0018): SUNY at Buffalo.
- Ellingwood, B. R. (2001). Earthquake risk assessment of building structures. *Reliability Engineering & System Safety*, 74(3), 251-262. doi: 10.1016/s0951-8320(01)00105-3
- Ellingwood, B. R., & Wen, Y.-K. (2005). Risk-benefit-based design decisions for low-probability/high consequence earthquake events in Mid-America. *Progress in Structural Engineering and Materials*, 7(2), 56-70. doi: 10.1002/pse.191
- Elwood, K. J. (2004). Modelling failures in existing reinforced concrete columns. *Canadian Journal of Civil Engineering*, 31(5), 846-859. doi: 10.1139/104-040
- Elwood, K. J., & Moehle, J. P. (2008). Dynamic shear and axial-load failure of reinforced concrete columns. *Journal of Structural Engineering*, 134(7), 1189-1198. doi: 10.1061/(asce)0733-9445(2008)134:7(1189)
- FEMA. (2011). Hazus.

- Freddi, F., Padgett, J. E., & Dall'Asta, A. (2012). Optimized Bilinear Probabilistic Models of the Seismic Response of a Low Ductility Reinforced Concrete Frame.
- Ghosh, J., & Padgett, J. E. (2011). Probabilistic seismic loss assessment of aging bridges using a component-level cost estimation approach. *Earthquake Engineering and Structural Dynamics*, 40(15), 1743-1761. doi: 10.1002/eqe.1114
- Goulet, C. A., Haselton, C. B., Mitrani-Reiser, J., Beck, J. L., Deierlein, G. G., Porter, K. A., & Stewart, J. P. (2007). Evaluation of the seismic performance of a code-conforming reinforced-concrete frame building - From seismic hazard to collapse safety and economic losses. *Earthquake Engineering and Structural Dynamics*, 36(13), 1973-1997. doi: 10.1002/eqe.694
- Hueste, M. B. D., & Wight, J. K. (1997). Evaluation of a four-story reinforced concrete building damaged during the Northridge Earthquake. *Earthquake Spectra*, 13(3), 387-414.
- Ibarra, L. F., Medina, R. A., & Krawinkler, H. (2005). Hysteretic models that incorporate strength and stiffness deterioration. *Earthquake Engineering and Structural Dynamics*, 34(12), 1489-1511. doi: 10.1002/eqe.495
- Kinali, K., & Ellingwood, B. R. (2007). Seismic fragility assessment of steel frames for consequence-based engineering: A case study for Memphis, TN. *Engineering Structures*, 29(6), 1115-1127. doi: 10.1016/j.engstruct.2006.08.017
- Kircher, C. A., Nassar, A. A., Kustu, O., & Holmes, W. T. (1997). Development of building damage functions for earthquake loss estimation. *Earthquake Spectra*, 13(4), 663-682.
- Krawinkler, H., Medina, R., & Alavi, B. (2003). Seismic drift and ductility demands and their dependence on ground motions. *Engineering Structures*, 25(5), 637-653. doi: 10.1016/s0141-0296(02)00174-8
- Liel, A. B. (2008). *Assessing the Collapse Risk of California's Existing Reinforced Concrete Frame Structures: Metrics for Seismic Safety Decisions*. (Doctor of Philosophy), Stanford University, Stanford, CA.
- Liel, A. B., Haselton, C. B., Deierlein, G. G., & Baker, J. W. (2009). Incorporating modeling uncertainties in the assessment of seismic collapse risk of buildings. *Structural Safety*, 31(2), 197-211. doi: DOI: 10.1016/j.strusafe.2008.06.002
- Lowes, L. N., Mitra, N., & Altoontash, A. (2004). A Beam-Column Joint Model for Simulating the Earthquake Response of Reinforced Concrete Frames: University of California, Berkeley.
- Maffei, J., Telleen, K., & Nakayama, Y. (2008). Probability-based seismic assessment of buildings, considering post-earthquake safety. *Earthquake Spectra*, 24(Copyright 2009, The Institution of Engineering and Technology), 667-699.
- McKenna, F., Mazzoni, S., Scott, M. H., Fenves, G. L., & al., e. (2006). Open System for Earthquake Engineering Simulation (OpenSees) OpenSees Command Language Manual. University of California, Berkeley, CA.

- Mitropoulou, C. C., Lagaros, N. D., & Papadrakakis, M. (2011). Life-cycle cost assessment of optimally designed reinforced concrete buildings under seismic actions. *Reliability Engineering and System Safety*, 96(10), 1311-1331. doi: 10.1016/j.ress.2011.04.002
- Neter, J., Kutner, M. H., Nachtsheim, C. J., & Wasserman, W. (1996). *Applied Linear Statistical Models* (Fourth Edition ed.): McGraw-Hill.
- NISEE. (2013). The Earthquake Engineering Online Archive. from <http://nisee.berkeley.edu/elibrary/>
- Padgett, J. E., & DesRoches, R. (2007). Sensitivity of Seismic Response and Fragility to Parameter Uncertainty. *Journal of Structural Engineering*, 133(12), 1710-1718. doi: 10.1061/(asce)0733-9445(2007)133:12(1710)
- Priestley, M. J. N. (1997). DISPLACEMENT-BASED SEISMIC ASSESSMENT OF REINFORCED CONCRETE BUILDINGS. *Journal of Earthquake Engineering*, 1(1), 157-192. doi: 10.1080/13632469708962365
- Ramamoorthy, S. K., Gardoni, P., & Bracci, J. M. (2006). Probabilistic demand models and fragility curves for reinforced concrete frames. *Journal of Structural Engineering*, 132(Compendex), 1563-1572.
- Serdar Kircil, M., & Polat, Z. (2006). Fragility analysis of mid-rise R/C frame buildings. *Engineering Structures*, 28(Compendex), 1335-1345.
- Shome, N. (1999). *Probabilistic Seismic Demand Analysis of Nonlinear Structures*. Stanford University, Stanford, CA.
- Tesfamariam, S., & Saatcioglu, M. (2008). Risk-based seismic evaluation of reinforced concrete buildings. *Earthquake Spectra*, 24(3), 795-821. doi: 10.1193/1.2952767
- Tubaldi, E., Barbato, M., & Dall'Asta, A. (2012). Influence of Model Parameter Uncertainty on Seismic Transverse Response and Vulnerability of Steel-Concrete Composite Bridges with Dual Load Path. *Journal of Structural Engineering*, 138(3), 363-374. doi: doi:10.1061/(ASCE)ST.1943-541X.0000456
- Vamvatsikos, D., & Allin Cornell, C. (2002). Incremental dynamic analysis. *Earthquake Engineering and Structural Dynamics*, 31(Compendex), 491-514.
- Vamvatsikos, D., & Fragiadakis, M. (2010). Incremental dynamic analysis for estimating seismic performance sensitivity and uncertainty. *Earthquake Engineering & Structural Dynamics*, 39(2), 141-163. doi: 10.1002/eqe.935
- Wen, Y. K., & Ellingwood, B. R. (2005). The role of fragility assessment in consequence-based engineering. *Earthquake Spectra*, 21(3), 861-877. doi: 10.1193/1.1979502
- Xue, Q., Wu, C. W., Chen, C. C., & Chou, W. Y. (2009). Post-earthquake loss assessment based on structural component damage inspection for residential RC buildings. *Engineering Structures*, 31(12), 2947-2953. doi: <http://dx.doi.org/10.1016/j.engstruct.2009.07.022>

Appendix A

Table A.1 - Parameters used in the OpenSees limit state material, axial limit curve, and shear limit curve for the column model.

Failure	Strain pinching factor	Force pinching factor	Integer for Curve type	Integer for Deformation type	Integer for Force type
Shear	0.5	0.4	2	2	0
Axial	0.5	0.5	1	2	2

Table A.2 - Unloading and pinching point parameters to be defined in the Pinching4 uniaxial material for zero length element located at joint intersection.³

Joint Location	Reloading displacement ratio	Reloading force ratio	Unloading force ratio
Interior	0.15	0.21	0.20
Exterior	0.15	0.15	0.10

³ Values are equal for positive and negative envelope curves.

Appendix B

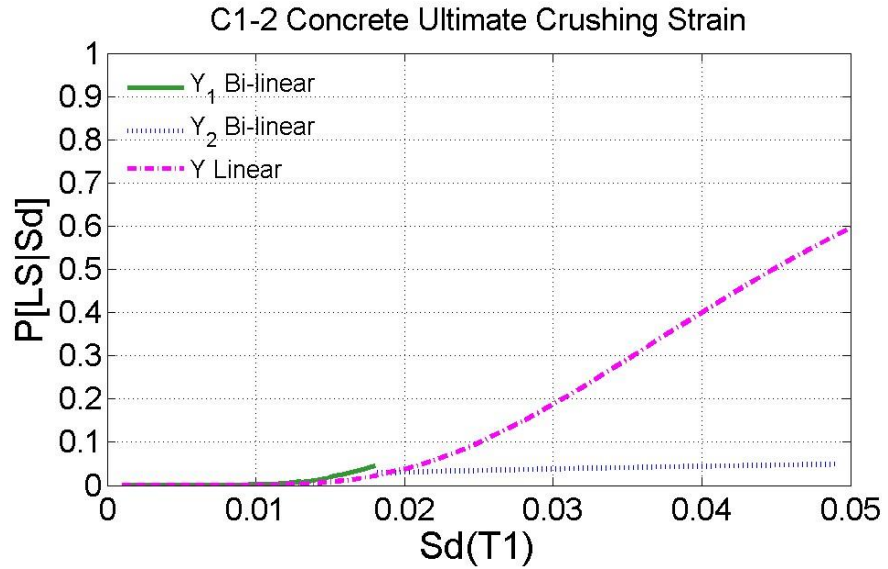


Figure B.1 - Linear and bilinear fragility curves for ultimate concrete crushing strain in column limit state.

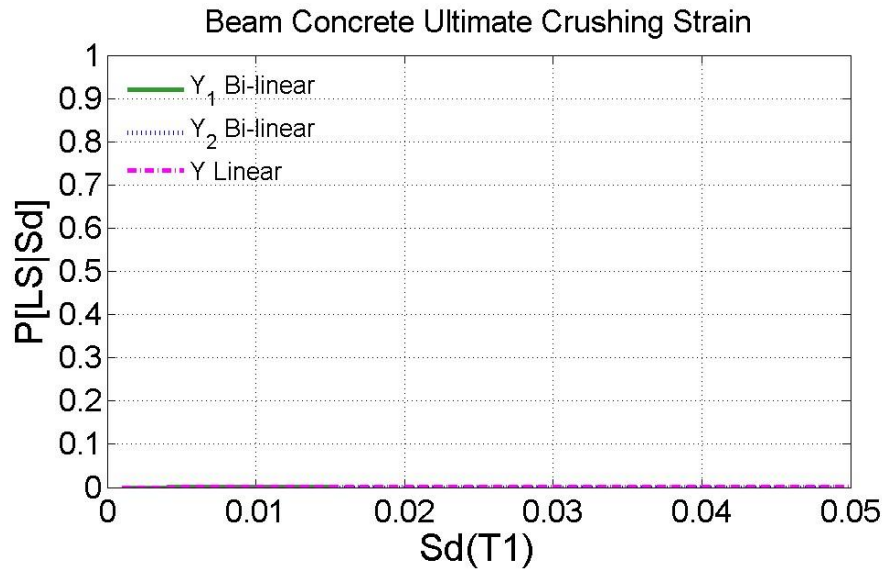


Figure B.2 - Linear and bilinear fragility curves for ultimate concrete crushing strain in beam limit state.

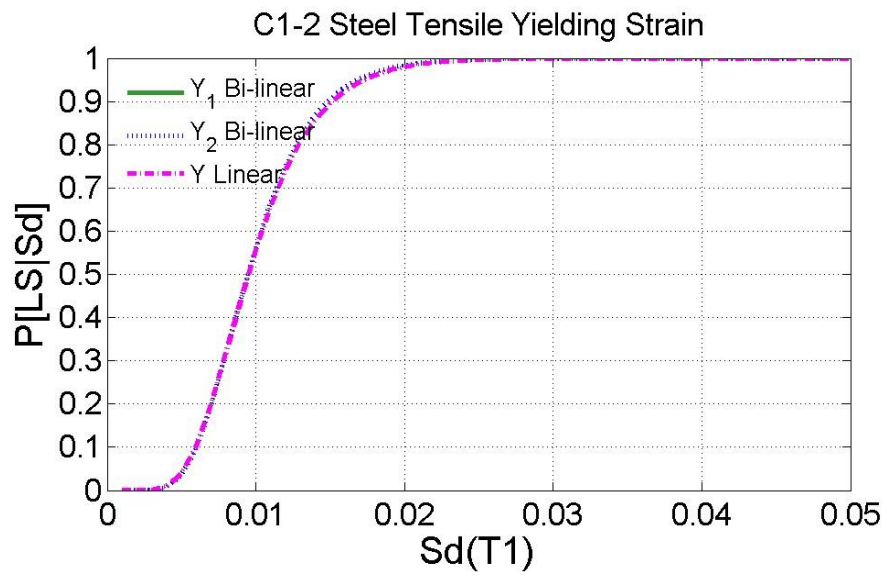


Figure B.3 - Linear and bilinear fragility curves for steel tensile yielding strain in column limit state.

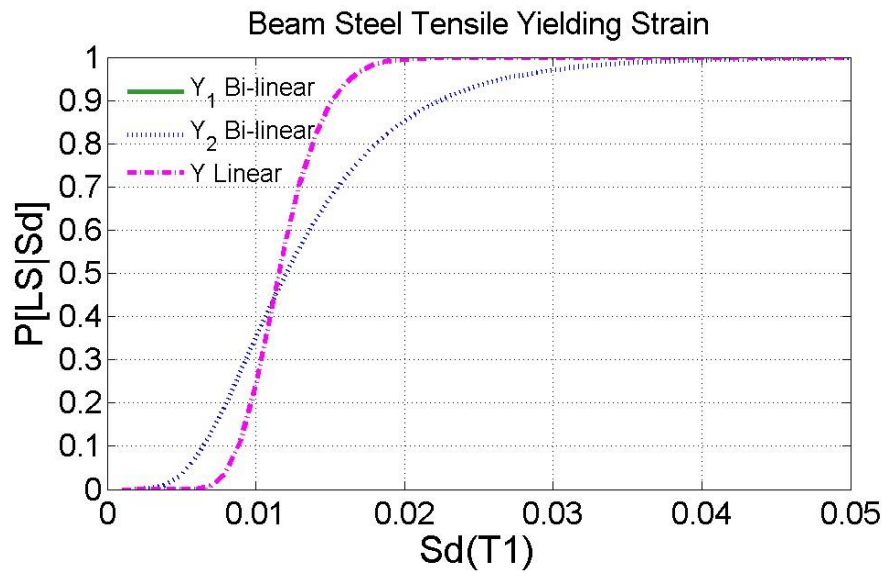


Figure B.4 - Linear and bilinear fragility curves for steel tensile yielding strain in beam limit state.

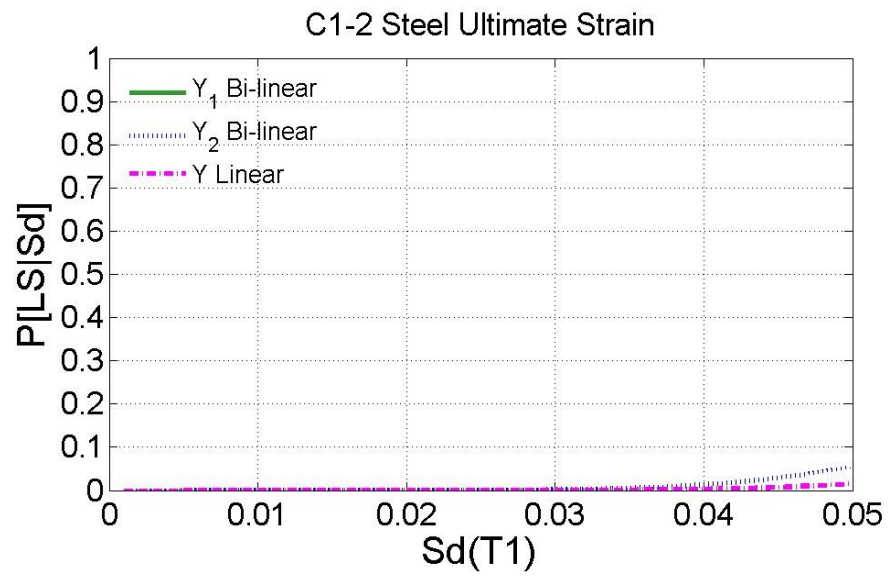


Figure B.5 - Linear and bilinear fragility curves for steel ultimate strain in column limit state.

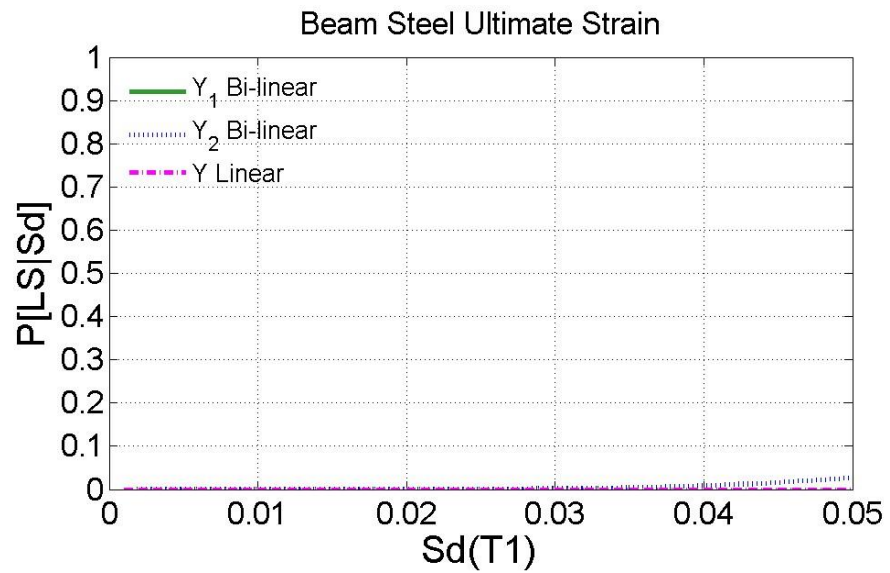


Figure B.6 - Linear and bilinear fragility curves for steel ultimate strain in beam limit state.

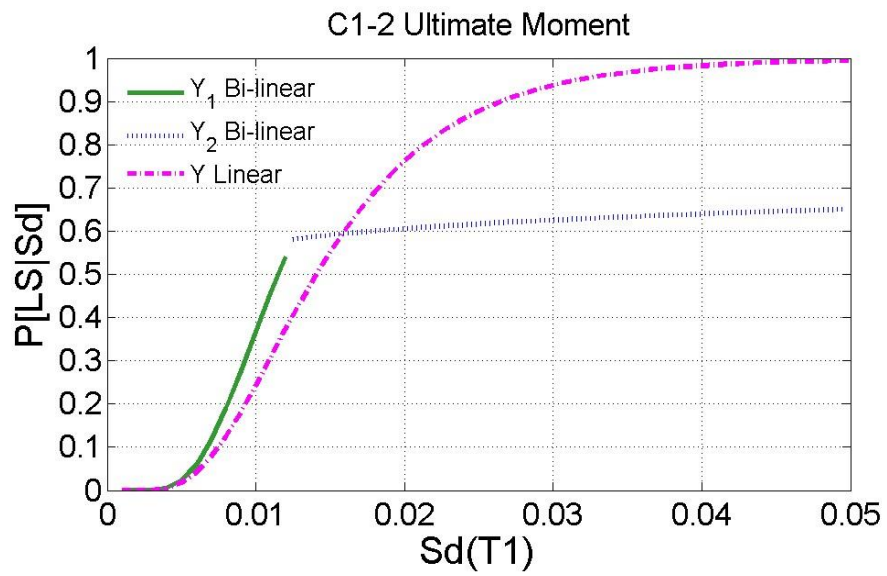


Figure B.7 - Linear and bilinear fragility curves for ultimate moment in column limit state.

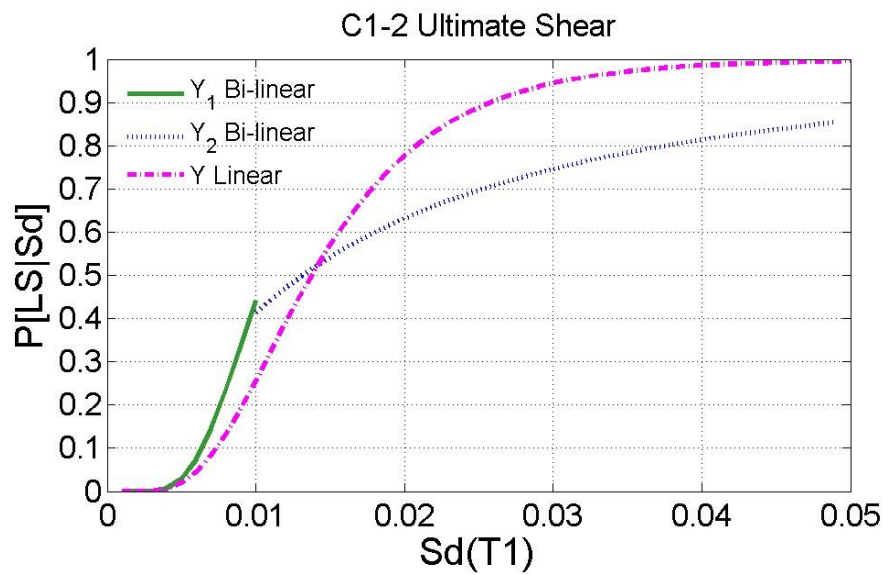


Figure B.8 - Linear and bilinear fragility curves for ultimate shear in column limit state.

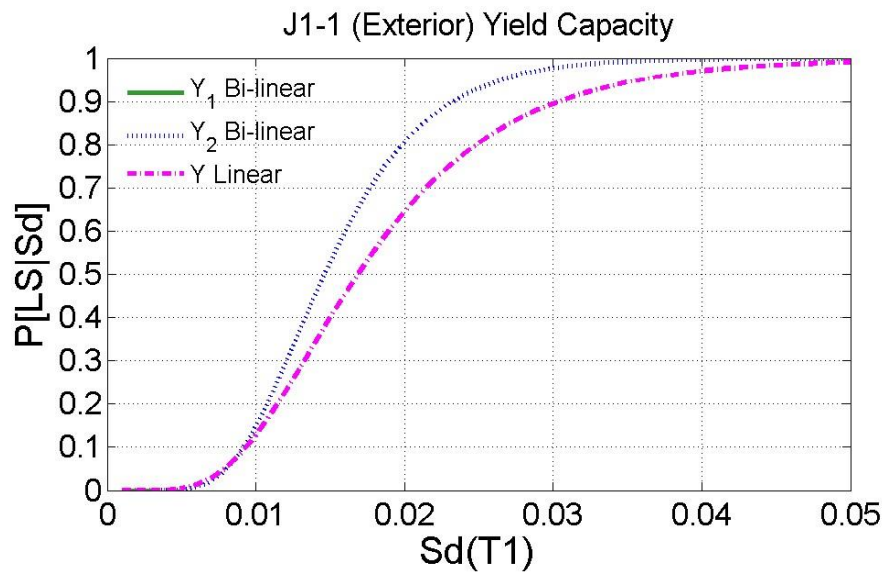


Figure B.9 - Linear and bilinear fragility curves for yielding strain in exterior joint limit state.

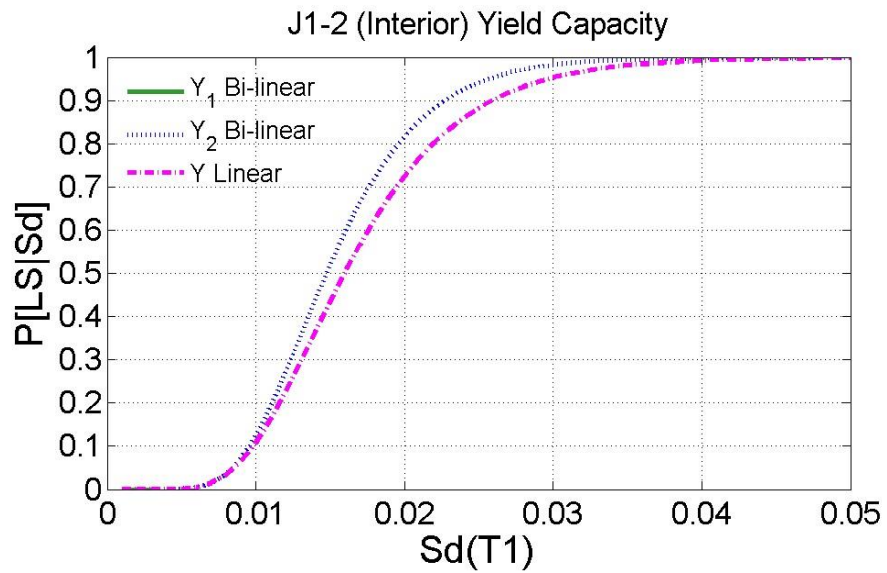


Figure B.10 - Linear and bilinear fragility curves for yielding strain in interior joint limit state.

Appendix C

SurveyMonkey Powered C x

https://www.surveymonkey.com/s/NEESRCBuildingDamageAssessment

The New Science Be... NCPDP - National C... Music PrePost Thursday

CONSENT FORM FOR PARTICIPATION IN RESEARCH Exit this survey

CONSENT FORM FOR PARTICIPATION IN RESEARCH

Study Title: NEESR-CR - Innovative Seismic Retrofits for Resilient Reinforced Concrete Buildings

Purpose of this Study:
This survey is conducted as a part of a NEESR-CR project. The purpose of this study is to identify repair models for damaged components of reinforced concrete buildings that have been subjected to earthquakes. The expertise solicited from engineering professionals will provide the research with valuable information on post-event tagging decisions, recommended repair strategies, and potential repair costs and timelines. The improved repair models will contribute to enhanced risk assessment and retrofit cost-benefit analysis of reinforced concrete buildings, in an effort to improve the seismic safety of these buildings through either traditional or innovative retrofit.

Procedures:
Following the Personal Information page, the participant will answer a set of questions pertaining repair of component damage shown in a Figure. In each Figure, groups of images are used to illustrate the type and level of component damage considered, as seen in different buildings subjected to earthquakes. For each Figure, you are asked for the tagging recommendation, repair strategy, estimated cost and duration of repair, as well as any additional comments. If you believe images under the same Figure are not repaired in the same manner, please feel free to comment in the space provided.

Compensation, Costs, & Confidentiality:
There will be no compensation or cost to you if you participate in this study. Your participation is greatly appreciated to support this research and its efforts to enhance the seismic safety of buildings. By participating in the study, you understand and agree that Rice University may be required to disclose your consent form, data and other personally identifiable information as required by law, regulation, subpoena or court order. Otherwise, your confidentiality will be maintained in the following manner: your data and consent form will be kept separate. By participating, you understand and agree that the data and information gathered during this study may be used by Rice University and published and/or disclosed by Rice University to others outside of Rice University. However, your name, address, contact information and other direct personal identifiers in your consent form will not be mentioned in any such publication or dissemination of the research data and/or results. If you have any questions about this study and your participation, please contact Dr. Jamie Padgett (jamie.padgett@rice.edu) and/or Blaine Fuselier (bjf@rice.edu).

Rights:
Your participation is voluntary. You are free to stop your participation at any point.
Your participation is greatly appreciated.

The expected duration of time for completion of this survey is 15-30 minutes.

Figures in the survey were captured from <http://nisee.berkeley.edu/elibrary/>

Do you consent to the information stated above?

YES NO

1 / 8 12%

Next

Figure C.1 - Consent form for participation in survey.

SurveyMonkey Powered C x

https://www.surveymonkey.com/s.aspx?sm=z58M7jShYDtAytCbInBKL8VVrqBKRCSezzyjnCCB0%3d

PERSONAL INFORMATION Exit this survey

Please provide the following information before continuing on to the survey:

Name (optional)

Organization

Title/Position

Address (optional)

Phone Number (optional)

Email (optional)

Rate your Post-Earthquake Level of Experience from 0 - 10 --> (0=no experience, 10=100+ hours of post-earthquake reconnaissance/repair)

Years of Professional Experience

2 / 8 25%

Powered by **SurveyMonkey**
Check out our [sample surveys](#) and create your own now!

Figure C.2 - Personal information page in survey.

SurveyMonkey Powered C x

← → <https://www.surveymonkey.com/s.aspx?sm=z58M7j5hYDtAyiTCbln8KL8VvrqBKRCSezzyujnCCB0%3d>

The New Science Be... NCPDP - National C... Music PrePost Thursday

REINFORCED CONCRETE COLUMN SHEAR Exit this survey




 

Figure 1: Column



Please provide answers most representative of the group identified in Figure 1, and if any case does not fit within the group you may identify it in the comment box:

1a. Suggested "tag" in post-earthquake evaluation:

Green
 Yellow
 Red (repairable)
 Red (demolition suggested)

1b. Recommended repair strategy to restore damaged component to its original state:

1c. Referring to your response in question (1b), approximate:

Duration of repair, including design (months):

Costs of repair (\$):

Comments referring to responses given in questions (1b) and (1c):

1d. What preventive retrofit measure(s) could have been taken, prior to the earthquake, to mitigate this type of damage?


Figure C.3 - Reinforced concrete column shear, part one, in survey.

SurveyMonkey Powered

https://www.surveymonkey.com/s.aspx?sm=z58M7j5hYDtAjjTCbInBKL8VrqBKRC5ezzyujnCCB0%3d

The New Science Be... NCPDP - National C... Music PrePost Thursday

Figure 2: Column



Please provide answers most representative of the group identified in Figure 2, and if any case does not fit within the group you may identify it in the comment box:

2. Will repair action responses given in Section 1 be the same for Figure 2?
 - If "yes" please proceed to next page
 - If "no" please answer the following questions for Section 2

yes
 no

2a. Suggested "tag" in post-earthquake evaluation:

Green Yellow Red (repairable) Red (demolition suggested)

2b. Recommended repair strategy to restore damaged component to its original state:

2c. Referring to your response in question (2b), approximate:

Duration of repair, including design (months):

Costs of repair (\$):

Comments referring to responses given in questions (2b) and (2c):

2d. What preventive retrofit measure(s) could have been taken, prior to the earthquake, to mitigate this type of damage?

3 / 8 38%

Prev Next

Powered by **SurveyMonkey**
 Check out our [sample surveys](#) and create your own now!

Figure C.4 - Reinforced concrete column shear, part two, in survey.

SurveyMonkey Powered C x

← → <https://www.surveymonkey.com/s.aspx?sm=z58M7j5hYDtAyiTCbInBKL8VvRqBKRC5ezzyujnCCB0%3d>

The New Science Be... NCPDP - National C... Music PrePost Thursday

REINFORCED CONCRETE SPALLING Exit this survey




 

Figure 1: Column

Please provide answers most representative of the group identified in Figure 1, and if any case does not fit within the group you may identify it in the comment box:

1a. Suggested "tag" in post-earthquake evaluation:

Green
 Yellow
 Red (repairable)
 Red (demolition suggested)

1b. Recommended repair strategy to restore damaged component to its original state:

1c. Referring to your response in question (1b), approximate:

Duration of repair, including design (months):

Costs of repair (\$):

Comments referring to responses given in questions (1b) and (1c):

1d. What preventive retrofit measure(s) could have been taken, prior to the earthquake, to mitigate this type of damage?


Figure C.5 - Reinforced concrete spalling of column in survey.

SurveyMonkey Powered

https://www.surveymonkey.com/s.aspx?sm=z58M7J5hYDtAjTcbInBKL8VVrqBKRCSzzyujnCCB0%3d

The New Science Be... NCPDP - National C... Music PrePost Thursday

Figure 2: Joint



Please provide answers most representative of the group identified in Figure 2, and if any case does not fit within the group you may identify it in the comment box:

2. Will repair action responses given in Section 1 be the same for Figure 2?
 - If "yes" please proceed to next page
 - If "no" please answer the following questions for Section 2

yes
 no

2a. Suggested "tag" in post-earthquake evaluation:

Green Yellow Red (repairable) Red (demolition suggested)

2b. Recommended repair strategy to restore damaged component to its original state:

2c. Referring to your response in question (2b), approximate:

Duration of repair, including design (months):

Costs of repair (\$):

Comments referring to responses given in questions (2b) and (2c):

2d. What preventive retrofit measure(s) could have been taken, prior to the earthquake, to mitigate this type of damage?

4 / 8 50%

Prev Next

Powered by **SurveyMonkey**
 Check out our [sample surveys](#) and create your own now!

Figure C.6 - Reinforced concrete spalling of joint in survey.

SurveyMonkey Powered C x


← → <https://www.surveymonkey.com/s.aspx?sm=z58M7j5hYDtAyiTCbInBKL8VvRqBKRC5ezzyujnCCB0%3d>

The New Science Be... NCPDP - National C... Music PrePost Thursday

REINFORCED CONCRETE JOINT Exit this survey

Figure 1: Joint




Please provide answers most representative of the group identified in Figure 1, and if any case does not fit within the group you may identify it in the comment box:

1a. Suggested "tag" in post-earthquake evaluation:

Green
 Yellow
 Red (repairable)
 Red (demolition suggested)

1b. Recommended repair strategy to restore damaged component to its original state:

1c. Referring to your response in question (1b), approximate:

Duration of repair, including design (months):

Costs of repair (\$):

Comments referring to responses given in questions (1b) and (1c):

1d. What preventive retrofit measure(s) could have been taken, prior to the earthquake, to mitigate this type of damage?


Figure C.7 - Reinforced concrete joint damage, part one, in survey.

SurveyMonkey Powered C x

← → <https://www.surveymonkey.com/s.aspx?sm=z58M7jShYDtAjjTCbInBKL8VrqbKRC5ezzyujnCCB0%3d>

The New Science Be... NCPDP - National C... Music PrePost Thursday

Figure 2: Joint



Please provide answers most representative of the group identified in Figure 2, and if any case does not fit within the group you may identify it in the comment box.

2. Will repair action responses given in Section 1 be the same for Figure 2?
 - If "yes" please proceed to next Page
 - If "no" please answer the following questions for Section 2

yes
 no

2a. Suggested "tag" in post-earthquake evaluation:

Green Yellow Red (repairable) Red (demolition suggested)

2b. Recommended repair strategy to restore damaged component to its original state:

2c. Referring to your response in question (2b), approximate:

Duration of repair, including design (months):

Costs of repair (\$):

Comments referring to responses given in questions (2b) and (2c):

2d. What preventive retrofit measure(s) could have been taken, prior to the earthquake, to mitigate this type of damage?

5 / 8 62%

Prev Next

Powered by [SurveyMonkey](#)
 Check out our [sample surveys](#) and create your own now!

Figure C.8 - Reinforced concrete joint damage, part two, in survey.

SurveyMonkey Powered C x

← → <https://www.surveymonkey.com/s.aspx?sm=z58M7j5hYDtAyiTCbInBKL8VvRqBKRC5ezzyujnCCB0%3d>

The New Science Be... NCPDP - National C... Music PrePost Thursday

REINFORCED CONCRETE COLUMN FLEXURE Exit this survey





 

Figure 1: Column

Please provide answers most representative of the group identified in Figure 1, and if any case does not fit within the group you may identify it in the comment box:

1a. Suggested "tag" in post-earthquake evaluation:

Green
 Yellow
 Red (repairable)
 Red (demolition suggested)

1b. Recommended repair strategy to restore damaged component to its original state:

1c. Referring to your response in question (1b), approximate:

Duration of repair, including design (months):

Costs of repair (\$):

Comments referring to responses given in questions (1b) and (1c):

1d. What preventive retrofit measure(s) could have been taken, prior to the earthquake, to mitigate this type of damage?

Figure C.9 - Reinforced concrete column flexure damage in survey.

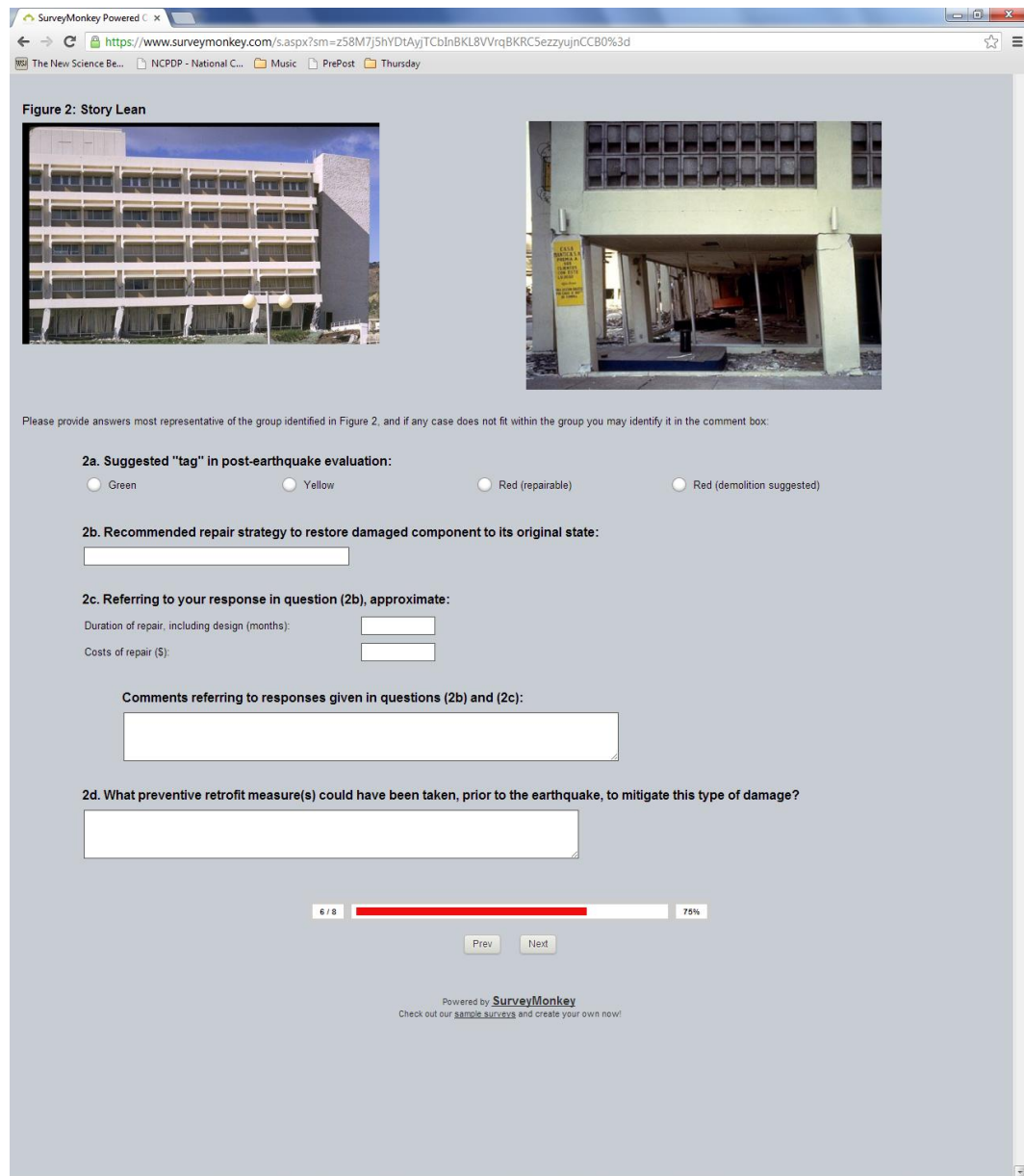


Figure C.10 - Reinforced concrete story lean observed damage in survey.

SurveyMonkey Powered C x

← → <https://www.surveymonkey.com/s.aspx?sm=z58M7j5hYDtAjyTCbInBKL8VrqbKRC5ezzyujnCCB0%3d>

The New Science Be... NCPDP - National C... Music PrePost Thursday

REINFORCED CONCRETE BEAM Exit this survey




 

Figure 1: Beam



Please provide answers most representative of the group identified in Figure 1, and if any case does not fit within the group you may identify it in the comment box:

1a. Suggested "tag" in post-earthquake evaluation:

Green Yellow Red (repairable) Red (demolition suggested)

1b. Recommended repair strategy to restore damaged component to its original state:

1c. Referring to your response in question (1b), approximate:

Duration of repair, including design (months):

Costs of repair (\$):

Comments referring to responses given in questions (1b) and (1c):

1d. What preventive retrofit measure(s) could have been taken, prior to the earthquake, to mitigate this type of damage?

Figure C.11 - Reinforced concrete beam damage, part one, in survey.

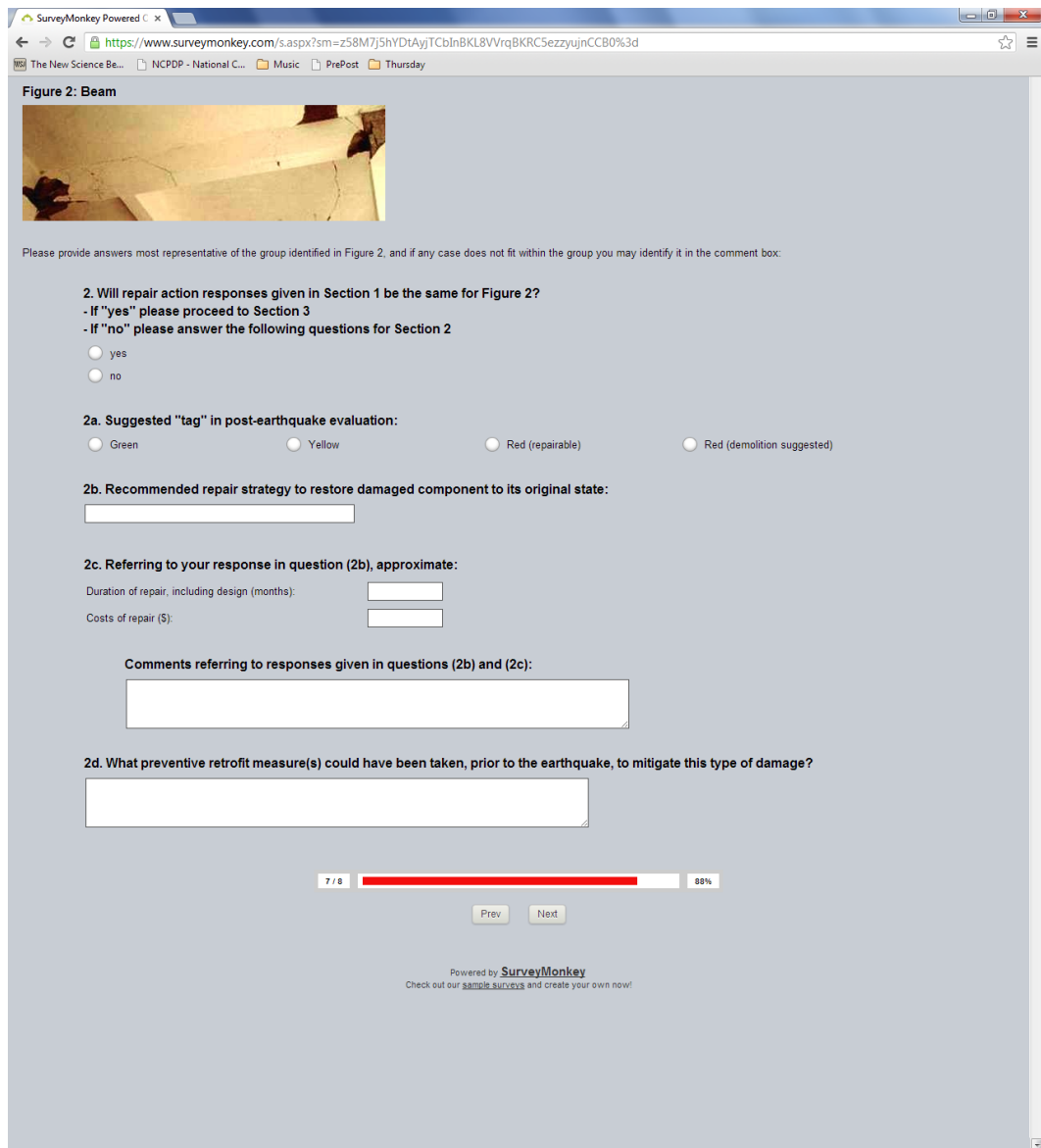



Figure C.12 - Reinforced concrete beam damage, part two, in survey.

SurveyMonkey Powered C x


https://www.surveymonkey.com/s.aspx?sm=z58M7j5hYDtAyiTCbInBKL8VvRqBKRC5ezzyujnCCB0%3d

The New Science Be... NCPDP - National C... Music PrePost Thursday


REINFORCED CONCRETE CORRELATIONS Exit this survey

RICE 


a) Column




b) Joint




c) Column



d) Beam



e) Beam



Focusing on the pictures above individually, would you classify any of the damaged components as "red" tagged upon individual inspection? (Mark all that apply)

a) b) c) d) e)

Excluding the damaged component(s) classified as "red" in the previous question, are there any combinations of damaged components, on one building, that would lead to a "red" tag?

	a)	b)	c)	d)	e)
1st Combination	<input type="checkbox"/>	<input type="checkbox"/>	<input type="checkbox"/>	<input type="checkbox"/>	<input type="checkbox"/>
2nd Combination	<input type="checkbox"/>	<input type="checkbox"/>	<input type="checkbox"/>	<input type="checkbox"/>	<input type="checkbox"/>
3rd Combination	<input type="checkbox"/>	<input type="checkbox"/>	<input type="checkbox"/>	<input type="checkbox"/>	<input type="checkbox"/>

Figure C.13 - Reinforced concrete correlations between damages in survey.